European Journal of Medicinal Chemistry 217 (2021) 113327

Contents lists available at ScienceDirect

European Journal of Medicinal Chemistry

journal homepage: http://www.elsevier.com/locate/ejmech

# Ring closure strategy leads to potent RIPK3 inhibitors

Shuwei Wu [a, 1], Chen Xu [a, 1], Kaijiang Xia [a], Yu Lin [a], Sheng Tian [a], Haikuo Ma [a], Yuting Ji [b, c], Fang Zhu [b, c], Sudan He [b, c, **], Xiaohu Zhang [a, *]

[a] Jiangsu Key Laboratory of Neuropsychiatric Diseases and College of Pharmaceutical Sciences, Soochow University, Suzhou, Jiangsu, 215123, PR China
[b] Center of Systems Medicine, Institute of Basic Medical Sciences, Chinese Academy of Medical Sciences & Peking Union Medial College, Beijing, Suzhou Institute of Systems Medicine, Suzhou, 215123, Jiangsu, PR China
[c] Cyrus Tang Hematology Center, Jiangsu Institute of Hematology and Collaborative Innovation Center of Hematology, Soochow University, Suzhou, 215123, PR China

ARTICLE INFO

*Article history:*
Received 6 November 2020
Received in revised form
10 February 2021
Accepted 19 February 2021
Available online 9 March 2021

*Keywords:*
Cell death
Inflammation
Necroptosis
RIPK1
RIPK3
Kinase

ABSTRACT

Necroptosis is a form of regulated necrotic cell death that is independent of caspases. Receptor-interacting protein kinase 3 (RIPK3) has been identified as a key regulator for necroptosis, and has been proposed as a potential therapeutic target for the treatment of diseases associated with necroptosis. In this report, we describe the design, synthesis, and evaluation of a series of novel RIPK3 inhibitors. The lead compound **38** exhibited potent activity ($EC_{50} = 0.42$ μM) in blocking TNFα, Smac mimetic and z-VAD (TSZ) induced cell death in HT-29 cells. Mechanistic studies showed that compound **38** bound to RIPK3 with high affinity ($K_d = 7.1$ nM), and inhibited RIPK3 kinase activity in a ADP-Glo functional assay. In addition, compound **38** displayed good selectivity over another necroptosis regulator RIPK1 ($K_d = 6000$ nM). Furthermore, compound **38** demonstrated excellent in vitro safety profiles with minimal inhibition of CYP isozymes and hERG potassium channel. Lastly, compound **38** efficiently blocked hypothermia and death in mice in the TNFα-induced systemic inflammatory response syndrome model.


## 1. Introduction

Necroptosis is a form of regulated, non-apoptotic cell death [1,2]. Necroptosis is tightly regulated by receptor-interacting protein kinase 1 (RIPK1) and RIPK3. Upon stimulation of necroptotic signals to death receptors, RIPK1 recruits RIPK3 through their RIP homotypic interaction motif (RHIM) domains to initiate the formation of the necrosome [3–5]. The necrosome serves as a molecular platform to active RIPK3, resulting in recruitment and phosphorylation of pseudokinase mixed lineage kinase domain-like protein (MLKL) [6–9]. The activated MLKL subsequently executes necroptosis by oligomerization and translocation to the plasma membrane, leading to the membrane rupture and the release of cellular contents [10–13]. Necroptosis is a necrotic, pro-inflammatory form of cell death that is involved in numerous human diseases including inflammatory diseases, degenerative diseases, ischemic infarction, and cancer [14–21]. As such, the key regulators of necroptosis, RIPK1, RIPK3, and MLKL, have been proposed as potential therapeutic targets for the treatment of the aforementioned diseases [22,23].

RIPK1 is the master regulator downstream of the death receptors, which is involved in determination of cell fate such as survival/inflammation or death (apoptosis and necroptosis) [24,25]. The multi-functional nature of RIPK1 complicates the interpretation of its role in necroptosis [26]. MLKL, on the other hand, is the executioner of necroptosis and represents an ideal target for necroptosis. However, as a pseudokinase, the enzyme activity (ATP binding and phosphorylation) and overall function (oligomerization and cell puncture) of MLKL is less tractable compares to RIPK3

*Abbreviations:* CYP, cytochrome P450; DCM, dichloromethane; DMF, *N*, *N*-dimethylformamide; DMPK, Drug Metabolism and Pharmacokinetics; DMSO, dimethyl sulfoxide; EA, ethyl acetate; HPLC, high performance liquid chromatography; hERG, human ether-a-go-go-related gene; IPA, isopropanol; LAH, lithium tetrahydroaluminate; *m*-CPBA, 3-chloroperbenzoic acid; NBS, *N*-bromosuccinimide; rt, room temperature; THF, tetrahydrofuran; TNFα, Tumor necrosis factor α; TsCl, *p*-Toluenesulfonyl chloride; Xphos, 2-(Dicyclohexylphosphino)-2,4,6-Triisopropylbiphenyl; XantPhos, 9,9-Dimethyl-4,5-bis(diphenylphosphino) xanthene.

* Corresponding author.
** Corresponding author. Center of Systems Medicine, Institute of Basic Medical Sciences, Chinese Academy of Medical Sciences & Peking Union Medial College, Beijing, Suzhou Institute of Systems Medicine, Suzhou, 215123, Jiangsu, PR China.
*E-mail addresses:* hesudan2018@163.com (S. He), xiaohuzhang@suda.edu.cn (X. Zhang).
[1] these authors contributed equally to this paper.

https://doi.org/10.1016/j.ejmech.2021.113327
0223-5234/

[8,27,28]. Moreover, it has been reported that necroptosis can proceed independent of RIPK1, leading to the assumption that RIPK3 may protect cell from a broader range of necroptotic pathologies than RIPK1 [29]. A number of RIPK3 inhibitors have been reported including the FDA approved drugs dabrafenib and ponatinib [30–32](Fig. 1). Dabrafenib and ponatinib are potent BRAF and BCR-ABL inhibitors, respectively. Their inhibition of RIPK3 was discovered as off-target activity, making them difficult starting points to selectively optimize RIPK3 activity. Very recently, two type-II RIPK3 inhibitors were reported [33,34](Fig. 1). Both compounds may need improvement for kinome-wide selectivity. For example, compound **2** is a potent RIPK3 inhibitor which is highly selective for RIPK3 over RIPK1 and RIPK2, but broader kinome scan showed compound **2** inhibited roughly 40 kinases out of 246 tested with an $IC_{50} < 1$ μM [34]. The seminal work on GSK′872 (Fig. 1) established RIPK3 as a drug target. GSK′872 was reported to be a potent and selective RIPK3 inhibitor which may induce apoptosis at high concentrations [35].

In pursuit of novel RIPK3 inhibitor, we decided to focus on the GSK′872 template since it was comprehensively characterized and showed good kinome wide selectivity. Our primary goal is to improve its moderate cellular potency. Ultimately, we want to understand the mechanism of RIPK3 inhibition induced apoptosis, and develop compounds with low cytotoxicity.

## 2. Design

In order to obtain promising RIPK3 inhibitors, structure-based drug design strategy was employed to guide our structural modification efforts. Briefly, GSK′872 was docked into the binding site of RIPK3 crystal complex (PDB ID: 4M69 [36]) from RCSB Protein Data Bank [37] by using *Glide* extra precision (XP) scoring function of Schrödinger 9.0 software package [38]. More detailed information for molecular docking procedure can be seen in our previous studies [39,40]. The binding conformation of GSK′872 predicted by *Glide* docking and key interaction patterns between GSK′872 and RIPK3 were depicted and analyzed. The computational results indicated that GSK′872 located in the ATP-binding site was a typical type I inhibitor, targeting the active DFG-in conformation of RIPK3 (Fig. 2a). Besides, GSK′872 had tight interactions with two key residues (Val36 and Asp161, Fig. 2b). In addition, we also found that the *6-(isopropylsulfonyl)quinoline* group of GSK′872 was solvent-exposed and in close range of residues including Val28, Gly31 and Ser147 in the binding site of RIPK3. Based on these observations, we hypothesized that the structural optimization on the quinoline group of GSK′872 for engagement of favorable interactions with these nearby residues may improve the inhibitory activity of rational-designed compounds. For the above-mentioned reasons, we formulated chemical modification/optimization plan as outlined in Fig. 3.

## 3. Chemistry

The synthesis of compounds **16**, **18** was displayed in Scheme 1. O-chloroaryl aldehyde was reacted with methyl 2-mercaptoacetate under basic conditions to provide **7**. Standard saponification of **7** resulted in carboxylic acid **8**, which was decarboxylated with copper powder to give **9**. Bromination of **9** with NBS led to **10**. Intermediates **9** and **10** were then oxidized by *m*-CPBA to afford the corresponding sulfones **11a**-**11b**. Reduction with iron powder led to the aromatic amines **12a**-**12b**, which were reacted with 5-(methoxymethylene)-2,2-dimethyl-1,3-dioxane-4,6-dione followed by cyclization in inert solvent at high temperature to provide the tricyclic pyridine analogues **14a**-**14b**. Treatment with $POCl_3$ followed by amino-benzothiazole provided advanced intermediates **15a**-**15b**. Final compound **16** was achieved by hydrogenation of **15a**. Final compound **18** was achieved by reacting **15b** with methanol followed by HCl hydrolysis. Compound **18** exists in tautomers as shown by $^1$H NMR (experimental section).

The synthetic approach of compounds **26**–**33** was shown in Scheme 2. Commercially available **19** was treated with sodium ethyl sulfonate followed by cyclization reaction in the presence of NaH, and then reacted with respective halogenated hydrocarbons to yield intermediates **20a**-**20c**. Reduction with iron powder resulted in the aniline analogues **21a**-**21c**. Bromination of compounds **21a**-**21c** with Oxone and NaBr afforded intermediates **22a**-**22c**, which were reacted with 5-(methoxymethylene)-2,2-dimethyl-1,3-dioxane-4,6-dione followed by cyclization at high temperature to yield tricyclic analogues **24a**-**24c**. Debromination was carried out in the presence of $H_2$, Pd/C to yield intermediates **25a**-**25c**, which were reacted with $POCl_3$ followed by substitution reactions with respective aromatic amines to form compounds

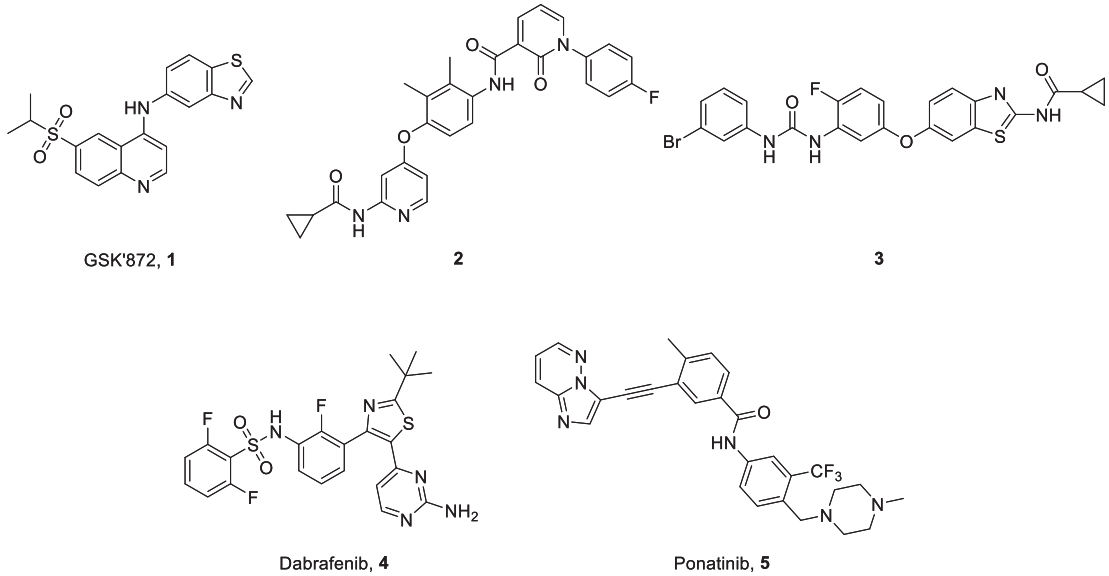


**Fig. 1.** Representatives of RIPK3 inhibitors reported in the literature.

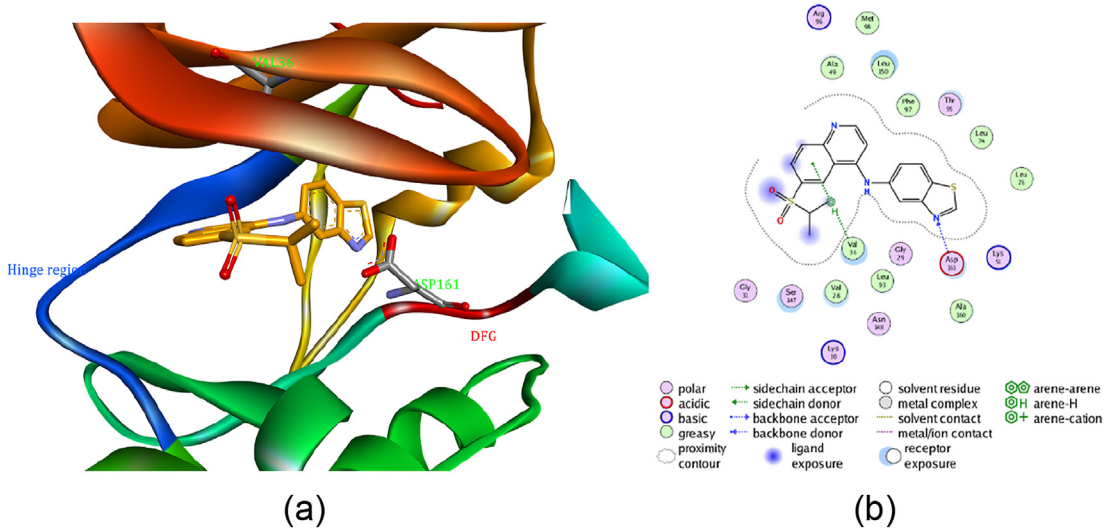


**Fig. 2.** (a). The predicted binding pose of GSK′872 based on 4M69 as RIPK3 docking template from *Glide* docking, the carbon atoms of GSK′872 are colored in golden, the residues of Hinge region are colored in blue, the DFG motif (Asp161-Phe162-Gly163) are colored in red and the favorable residues are labeled in green; (b). Interaction patterns between GSK′872 and key residues in the binding site of RIPK3.

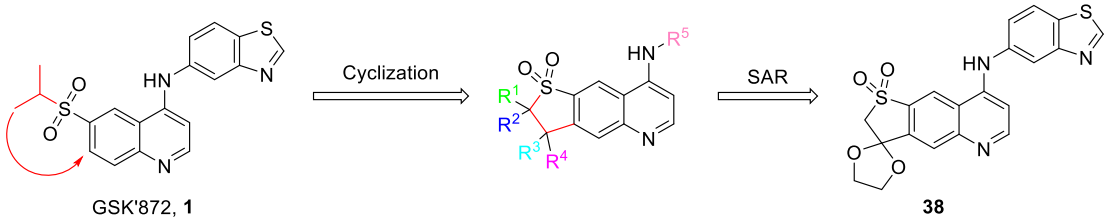


**Fig. 3.** Proposed SAR study plan.

**26**–**33**.

The synthesis of compounds **34**–**39** was performed as shown in Scheme 3. Nucleophilic reaction with ketone **26** was carried out by hydride provided by $NaBH_4$ or carbanions provided by respective Grignards to yield corresponding secondary alcohol **34**, or tertiary alcohols **35**–**36**. Wittig reaction with ketone **26** provided final compound **37**. A combination of Michael addition and substitution reaction between **15b** and ethylene glycol/methyl ethylene glycol yielded compounds **38** and **39**, respectively.

Compound **47** was prepared as described in Scheme 4. Palladium catalyzed coupling of intermediate **10** with methyl acrylate provided compound **40**. The combination of $NaBH_4$ and $AlCl_3$ reduced both of the nitro and the ester to provide primary alcohol **41**. Treatment of **41** with *m*-CPBA converted the amino to nitro while oxidized the sulfur to sulfone to give intermediate **42**. The sulfone **42** facilitated intramolecular cyclization under basic conditions to give **43**. Following similar steps presented in Scheme 1, intermediate **43** was converted to the target compound **47**.

The synthesis of compound **61** was performed as shown in Scheme 5. Commercially available **48** was reacted with dimethyl carbonate under basic conditions to form compound **49**, which was reacted with ((chloromethoxy)methyl)benzene to achieve intermediate **50**. Reduction of **50** with LAH yielded **51**. One of the hydroxyls was reacted with TsCl to form a leaving group, facilitating an intramolecular cyclization to give intermediate **52**. Debenzylation of **52** with $H_2$, Pd/C provided **53**, which was converted to **54** by Appel reaction. Nitration reaction was accomplished with concentration $H_2SO_4$ and $HNO_3$ to afford **55**, which was converted to **56** via an intramolecular cyclization with $Na_2S.9H_2O$. Intermediate **60** was obtained by similar reactions presented in Scheme 1, which was reacted with trifluoromethanesulfonic anhydride followed by Buchwald coupling with 1-benzothiophen-5-amine to form the target product **61**.

## 4. Results and discussion

### 4.1. Structure-activity-relationship of synthesized compounds

We used a cell based assay to evaluate the *anti*-necroptosis activity of synthesized compounds. Human colon cancer HT-29 cells were treated with TNFα, Smac mimetic and z-VAD (a pan caspase inhibitor) to induce necroptotic cell death (the TSZ induced cell death). Cell viability was analyzed by monitoring ATP levels. The *anti*-necroptosis activity of compound was evaluated by pre-incubation of compound with the TSZ treated cells and its ability to rescue cells from TSZ induced death was the readout. Compounds were also run a concentration gradience without TSZ treatment to assess their cellular toxicity. We excluded compounds which showed significant cellular toxicity at 20 μM concentration (>30% cell death). This is an efficient assay with stable readout and good throughput. As compounds with enhanced potency are identified, we would expand the necroptosis assay to include rodent cells, and more mechanistic based assays such as kinase binding and functional assays. As shown in Table 1, cyclization of the sulfone group to form a simple 5-member ring led to compound **16** (2.28 μM), which showed *anti*-necroptosis activity comparable to GSK′872 (1.51 μM). Further functionalization of the 5-member ring with a hydrophilic carbonyl improved the novelty of the

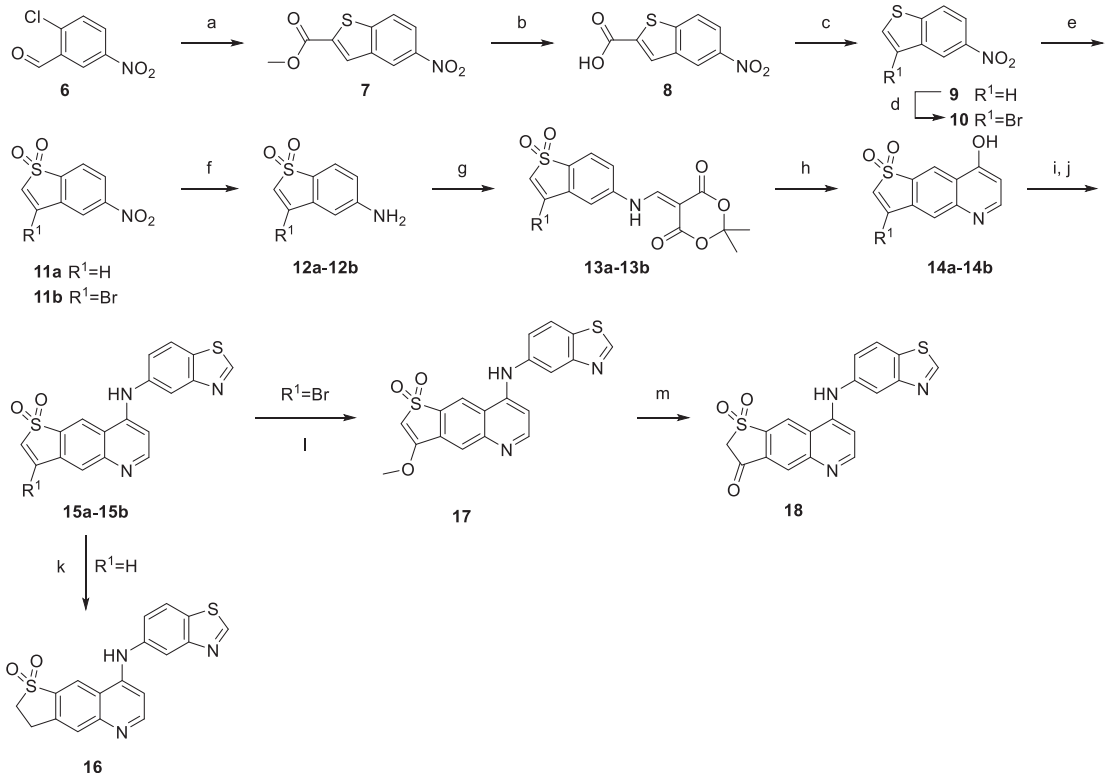


**Scheme 1.** Reagents and conditions: (a) methyl 2-mercaptoacetate, $K_2CO_3$, DMF, r.t, overnight,; (b) NaOH, MeOH, $H_2O$, 70 °C, 4 h; (c) Cu, quinoline, 170 °C, 4 h; (d) NBS, DMF, 60 °C, 3 h; (e) *m*-CPBA, DCM, r.t, overnight; (f) Fe, $NH_4Cl$, EtOH, $H_2O$, 85 °C, 2 h; (g) 5-(methoxymethylene)-2,2-dimethyl-1,3-dioxane-4,6-dione, EtOH, r.t, 30 min; (h) $Ph_2O$, 240 °C, 5 min; (i) $POCl_3$, 110 °C, 2 h; (j) benzo[*d*]thiazol-5-amine, EtOH, conc. HCl, reflux, 1 h; (k) $H_2$, Pd/C, $CH_3OH$, r.t, overnight; (l) $Cs_2CO_3$, $CH_3OH$, r.t, 20 h; (m) $CH_3CN$, conc. HCl, 80 °C, overnight.

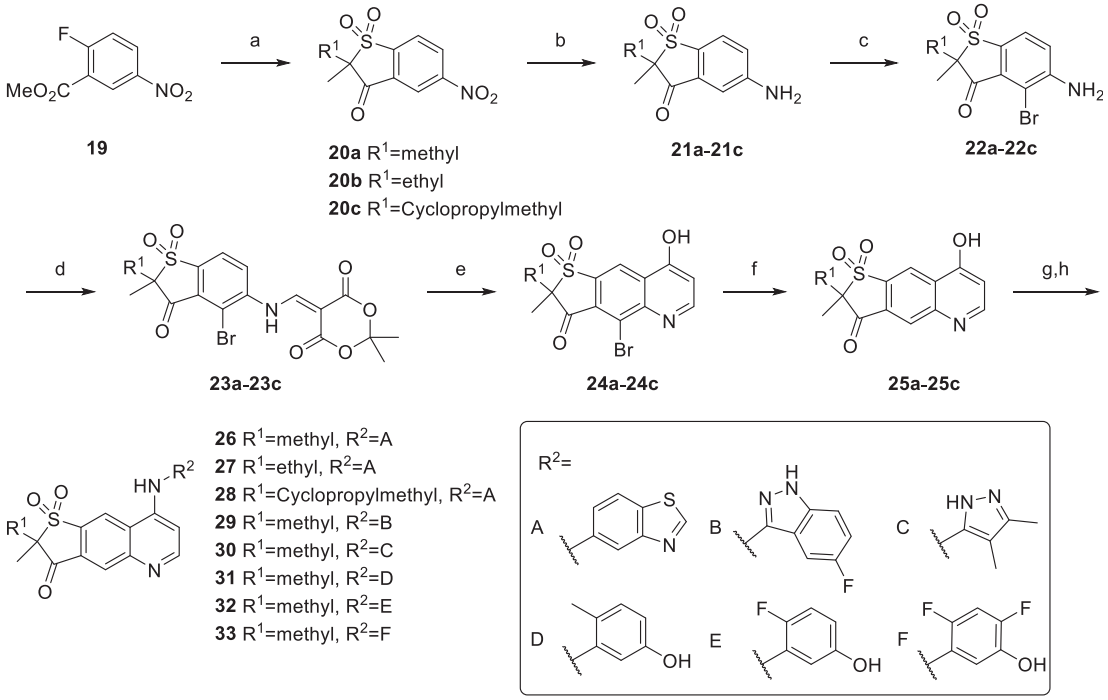


**Scheme 2.** Reagents and conditions: (a) 1) $EtSO_2Na$, DMSO, r.t, overnight; 2) NaH, 0 °C to r.t, 3 h; 3) $R^1$-Br, r.t, 5 h; (b) Fe, $NH_4Cl$, EtOH, $H_2O$, 85 °C, 2 h; (c) Oxone, NaBr, $CH_3OH/H_2O$, r.t, 4 h; (d) 5-(methoxymethylene)-2,2-dimethyl-1,3-dioxane-4,6-dione, EtOH, r.t, 30 min; (e) $Ph_2O$, 240 °C, 5 min; (f) $H_2$, Pd/C, TEA, i-PrOH, $H_2O$, r.t 1.5 h; (g) $POCl_3$, 110 °C, 2 h; (h) $R^2$-$NH_2$, EtOH, conc. HCl, reflux, 1 h.

template (compound **18**, 3.81 μM). The methylene between the sulfone and the carbonyl is fairly acidic, which can be easily functionalized by alkylation reaction. Dimethyl analogue compound **26** (2.23 μM) displayed comparable activity to GSK'872,

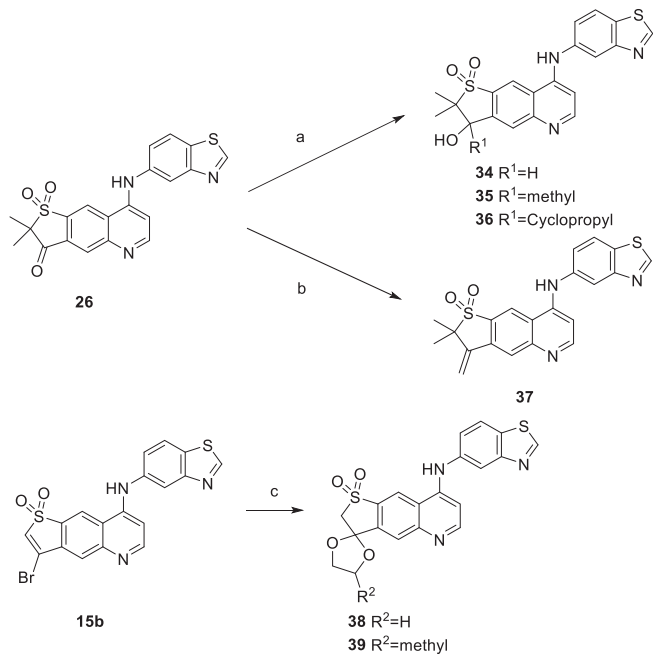


**Scheme 3.** Reagents and conditions: (a) 1) $NaBH_4$, $CH_3OH$, $CH_2Cl_2$, 30 min for **34**. 2) $R^1$-MgBr, THF, 0 °C - r.t, 1 h for **35**, **36**; (b) Methyltriphenyl phosphonium bromide, n-BuLi, THF, −78 °C to r.t; (c) $Cs_2CO_3$, Ethylene glycol, 60 °C, 5 h for **38**; $Cs_2CO_3$, propane-1,2-diol, 60 °C, 5 h for **39**.

however, increased size (compounds **27** and **28**, >20 μM) was not well tolerated at this position. We chose compound **26** as the prototype for the next round of exploration (see Table 2).

In order to investigate the back pocket interactions, we carefully selected a small size of aromatic fragments based on our docking study and structure-activity information reported in the literation. 5-fluoro-1H-indazol-3-amine and 3-amino-4,5-dimethyl pyrazole were successfully applied to improve potency and reduce hERG activity in related programs [41,42], but unfortunately were not active in our template (compounds **29** and **30**, >20 μM). The aminophenol fragments led to a number of potent compounds (compounds **31**, **32**, **33**; 0.52, 0.33, 1.03 μM, respectively), however, these compounds exhibited significant cellular toxicity (>30% cell death at 20 μM concentration) in the screen assay, making them unsuitable for further optimization. Overall, the amino-benzothiazole remained to be the favorable back pocket substituent for additional structure-activity investigation.

Having established the amino-benzothiazole as the best structural element for the back pocket, we decided to further explore modifications on the carbonyl of the cyclic sulfone ring. According to our docking study described in the above section, this position faces solvent, we therefore expected more structure diversity to be tolerated. Reduction of the carbonyl gave compound **34** (2.19 μM), which showed comparable activity to GSK′872. Nucleophilic addition of the carbonyl with carbanions led to compounds **35** and **36**, which unfortunately were inactive. Wittig reaction introduced exocyclic ethene **37** (1.03 μM), which was as potent as GSK′872. Conversion of the carbonyl into ketal with ethylene glycol led to compound **38** (0.42 μM), which was three times more potent than GSK′872 in blocking TSZ induced cell death in TH-29 cells. The docking pose predicted by *Glide* docking of compound **38** and key interactions between compound **38** and RIPK3 were analyzed. As shown in Fig. 4, additional interactions, three hydrogen bonds were formed between modified function group (*2H-spiro[thieno[2,3-g] quinoline-3,2′- [1,3]dioxolane] 1,1-dioxide*) and Ser102 residue in the solvent-exposed region of RIPK3. This finding may explain why compound **38** has better inhibitory activity than GSK′872 to some extent. More importantly, compound **38** did not exhibited any cellular toxicity in HT-29 cell up to 20 μM. This is in stark contrast to the amino-phenol analogues. Addition of a methyl on the ketal (compound **39**, 1.07 μM) did not improve activity. Removal of an oxygen from the ketal was detrimental to activity (compound **47**, 3.96 μM). In an attempt to move oxygen to face solvent, compound **61** was proposed. Compound **61** was devoid of the potential instability of **38** in strong acidic conditions and chirality associated with **39** and **47**. The synthesis of compound **61** proved challenging and a dedicated synthetic sequence was developed (Scheme 5). To

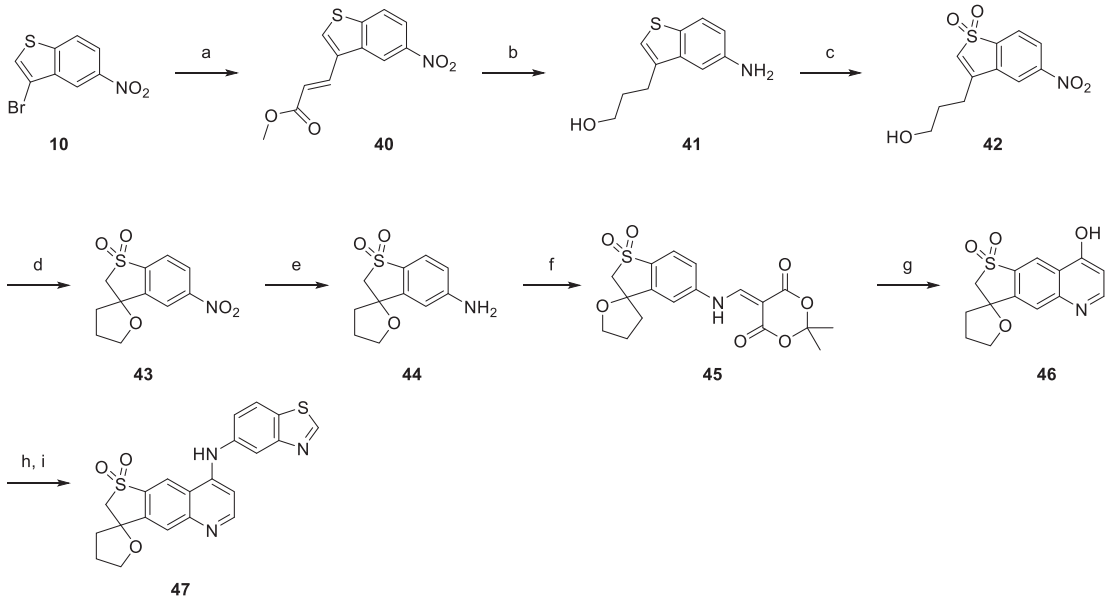


**Scheme 4.** Reagents and conditions: (a) methyl acrylate, $Pd(OAc)_2$, XPhos, $NaHCO_3$, DMF, 120 °C, 4 h; (b) $NaBH_4$, $AlCl_3$, THF, 2 d; (c) *m*-CPBA, DCM, overnight; (d) $CH_3OH$, $Cs_2CO_3$, r.t, 2 h; (e) Fe, $NH_4Cl$, EtOH/$H_2O$, 80 °C, 1 h; (f) 5-(methoxymethylene)-2,2-dimethyl-1,3-dioxane-4,6-dione, EtOH, r.t, 20 min; (g) $Ph_2O$, 240 °C, 5 min; (h) $POCl_3$, 110 °C, 2 h; (i) benzo[*d*] thiazol-5-amine, EtOH, conc. HCl, reflux, 2 h.

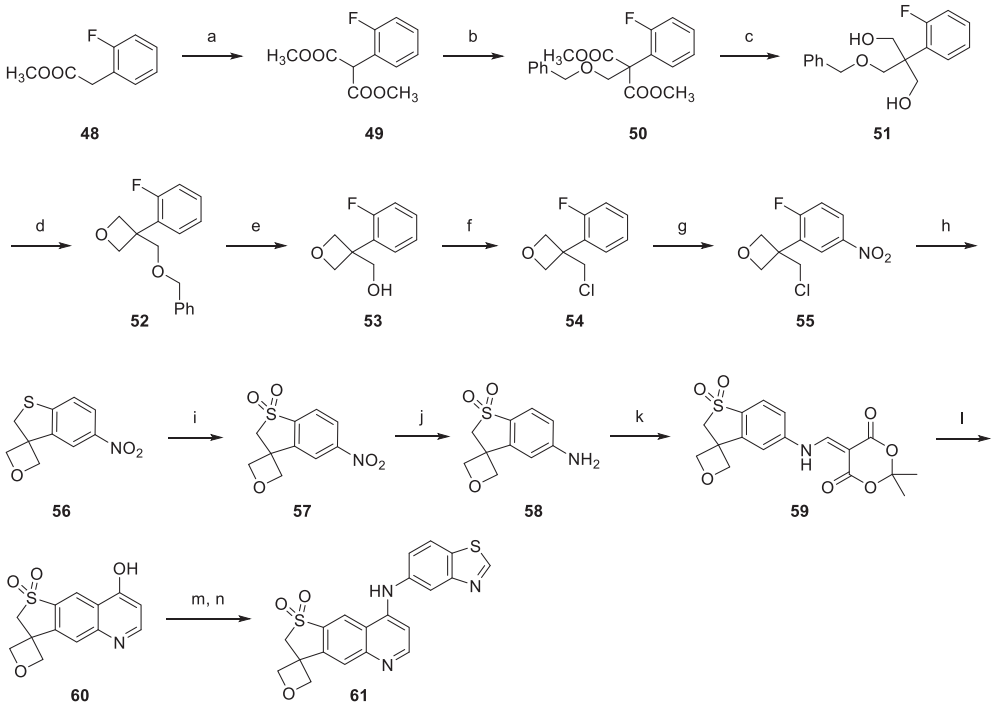


**Scheme 5.** Reagents and conditions: (a) dimethyl carbonate, NaH, THF, 70 °C, overnight; (b) ((chloromethoxy)methyl)benzene, $Cs_2CO_3$, DMF, r.t, 1 h; (c)LAH, THF, 0 °C to r.t, 2 h; (d) 1) n-BuLi, TsCl, THF, 0 °C, 10 min; 2) n-BuLi, 55 °C, overnight; (e) $H_2$, Pd/C, $CH_3OH$, r.t, 12 h; (f) $CCl_4$, $PPh_3$, 90 °C, 24 h; (g) $H_2SO_4$, $HNO_3$, 0 °C to r.t, 5 min; (h) $Na_2S.9H_2O$, DMSO, r.t, 3 h; (i) *m*-CPBA, DCM, r.t overnight; (j) Fe, $NH_4Cl$, EtOH/$H_2O$, 80 °C, 2 h; (k) 5-(methoxymethylene)-2,2-dimethyl-1,3-dioxane- 4,6-dione, EtOH, r.t, 20 min; (l) $Ph_2O$, 240 °C, 5 min; (m) $(CF_3SO_2)_2O$, DCM, Pyridine, r.t, 30 min; (n) benzo[*d*]thiazol-5-amine, $Pd_2(dba)_3$, Xantphos, $Cs_2CO_3$, dioxane, 100 °C, 1 h.

**Table 1**
SAR for $R^1$, $R^2$, $R^3$, $R^4$.

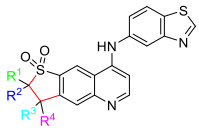

| Compd. | Structure | $EC_{50}$HT-29 (μM)[a] | M.W. | clogP[b] |
|---|---|---|---|---|
| **16** | 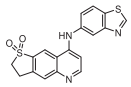 | 2.28 ± 0.54 | 367.4 | 3.83 |
| **18** | 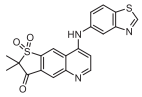 | 3.81 ± 0.57 | 381.4 | 3.17 |
| **26** | 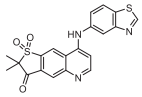 | 2.23 ± 0.15 | 409.5 | 3.98 |
| **27** | 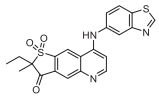 | >20 | 422.5 | 4.48 |
| **28** | 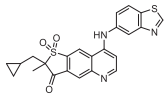 | >20 | 449.5 | 4.75 |
| **1** | | 1.51 ± 0.14 | 383.5 | 4.16 |

[a] Human HT-29 cells were pretreated with DMSO or the test compound and then stimulated with TNFα (20 ng/mL), Smac mimetic (100 nM), and z-VAD (20 μM) (TSZ) for 40 h. The inhibition of TSZ-induced necroptosis in HT-29 cells is presented as geometric mean values of at least two runs ± the standard error measurement (SEM). [b] Calculated by Molinspiration.

**Table 2**
SAR for R.[5].

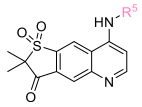

| Compd. | $R^5$ | $EC_{50}$HT-29 (μM)[a] | M.W. | clogP[b] |
|---|---|---|---|---|
| **29** |  | >20 | 410.4 | 2.55 |
| **30** |  | >20 | 370.4 | 2.67 |
| **31** |  | 0.43 ± 0.09[c] | 382.4 | 3.47 |
| **32** |  | 0.33 ± 0.01[c] | 386.4 | 3.18 |
| **33** |  | 1.03 ± 0.31[c] | 404.4 | 3.54 |
| **1** | | 1.51 ± 0.14 | 383.5 | 4.16 |

[a] Inhibition of TSZ-induced necroptosis in HT-29 cells. [b] Calculated by Molinspiration. [c] Significant cellular toxicity at 20 μM concentration (>30% cell death).

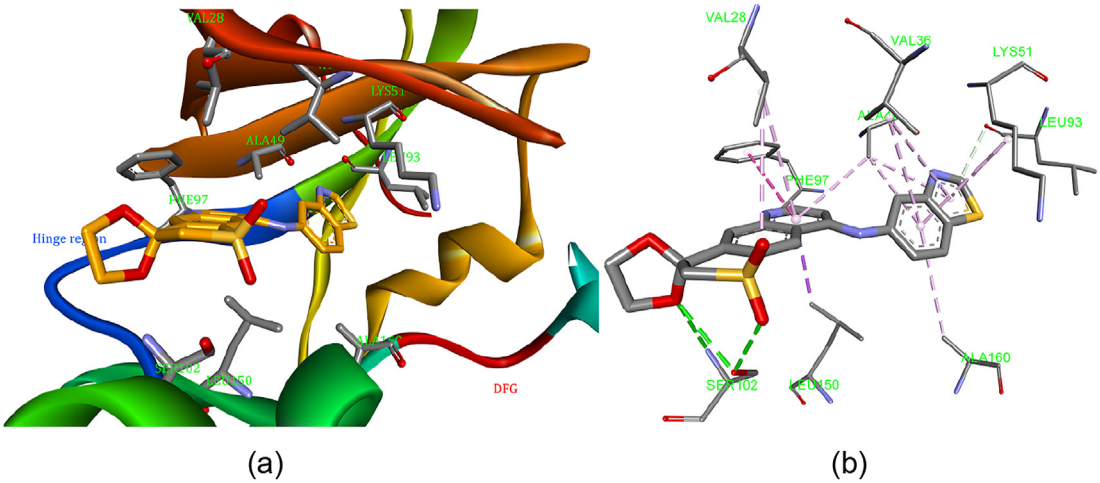


**Fig. 4.** (a). The predicted binding pose of compound **38** based on 4M69 as RIPK3 docking template from *Glide* docking, the carbon atoms of compound **38** are colored in golden, the residues of Hinge region are colored in blue, the DFG motif (Asp161-Phe162-Gly163) are colored in red and the favorable residues are labeled in green; (b). Interaction patterns between compound **38** and key residues in the binding site of RIPK3.

our disappointment, compound **61** was inactive in rescuing HT-29 cells from TSZ necroptosis stimuli. Overall, the docking study was helpful in the structure-activity relationship exploration. However, some of the subtle difference, especially toward to solvent-exposed region of the tricyclic template, could not be fully rationalized.

Collectively, structural modifications on the back pocket and the newly formed sulfone ring led to numerous compounds with improved *anti*-necroptosis activity. (e.g., compounds **31**, **32**, **33**, and **38**, 0.52, 0.33, 1.03, and 0.42 μM, respectively). The significant cellular toxicity displayed by compounds **31**, **32**, and **33** in the screening assay deemed them unsuitable to be further optimized. On the other hand, compound **38** was potent and exhibited no sign of cellular toxicity up to 20 μM in the screening assay. Moreover, compound **38** displayed moderate physicochemical properties (M.W., 425; clogP, 3.5) and represented a very novel scaffold in the RIPK3 patent space. Based on these merits, compound **38** was selected for mechanistic testing (see Table 3).

### 4.2. Mechanistic evaluation of lead compound 38

The inhibition of TNFα, Smac mimetic and z-VAD induced necroptotic death in human colon cancer cells is a good indication of *anti*-necroptosis activity of compounds in human (Fig. 5a, *anti*-necroptosis effects of compound **38**, 0.42 μM; GSK′872, 1.51 μM in HT-29 cells). We next tested compound **38** in mouse cells. Compound **38** efficiently inhibited TNF-induced necroptosis in mouse embryonic fibroblasts (MEFs) with an $EC_{50}$ of 0.54 μM (Fig. 5b), while GSK′872 displayed an $EC_{50}$ of 2.51 μM under the same experimental conditions. These results demonstrated that **38** is an inhibitor of TNF-induced necroptosis in both human and mouse cells. The consistent activity of compound **38** in human and mouse cells deemed it suitable to be tested in preclinical species for efficacy as a surrogate of human diseases. TNF-induced necroptosis propagates through RIPK1/RIPK3/MLKL. Although compound **38** was derived from GSK′872, a well characterized RIPK3 inhibitor, we sought to determine whether compound **38** directly targeted RIPK3 or RIPK1. Compound **38** was subjected to KINOMEscan to

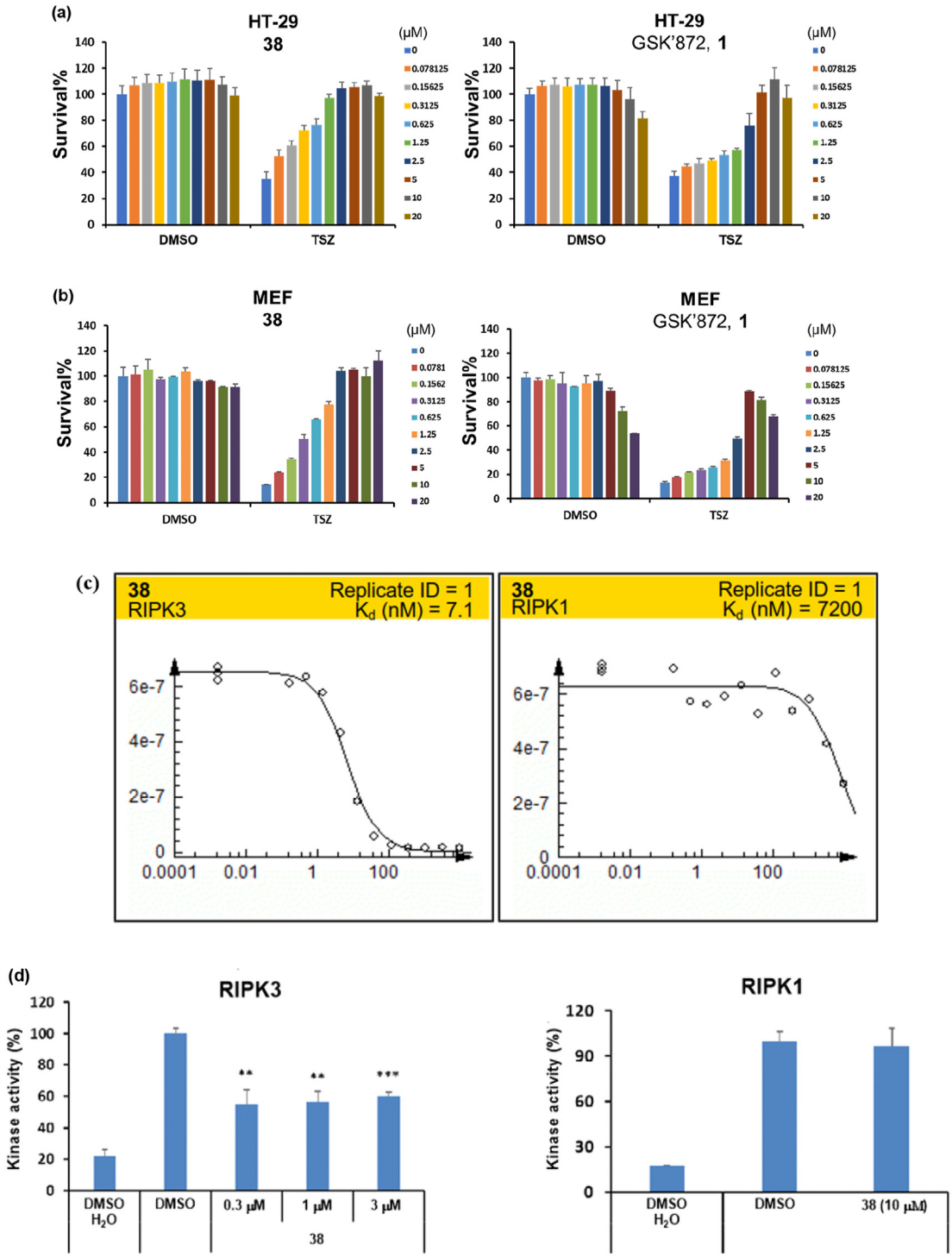


**Fig. 5.** Compound **38** is a potent RIPK3 inhibitor, but is inactive to RIPK1. HT-29 cells (a) and MEFs (b) were pretreated with DMSO, compound **38**, or **1** and then stimulated with TNFα (20 ng/mL), Smac mimetic (100 nM) and z-VAD (20 μM) (TSZ) for 40 h; (c) The binding affinity of the test compounds on RIPK1 and RIPK3 kinases was detected by a KINOMEscan assay. (d) The functional kinase inhibition of test compounds was detected by the ADP-Glo kinase assay.

determine its binding to RIPK1 and RIPK3. As shown in Fig. 5c, compound **38** displayed high binding affinity to RIPK3 ($K_d$ = 7.2 ± 0.05 nM, one replicate curve was shown) while only marginal binding affinity to RIPK1 ($K_d$ = 5950 ± 1250 nM, one replicate curve was shown). In consistent to the binding data, compound **38** significant reduced the RIPK3 kinase functional activity in the ADP-Glo kinase assay at 0.3 μM concentration, while exhibited no inhibition of RIPK1 kinase function even at 10 μM concentration (Fig. 5d). MLKL is the executioner of necroptosis and is a potential molecular target of compound **38**. We therefore used enforced dimerization/polymerization of MLKL to test if compound **38** inhibited MLKL dimerization. Compound **38** did not block this MLKL polymerization induced necroptosis, suggested that MLKL is not the molecular target for compound **38** (data not shown). We

**Table 3**
SAR for $R^1$, $R^2$, $R^3$, $R^4$.

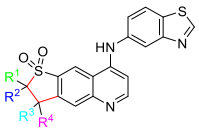

| Compd. | Structure | $EC_{50}$HT-29 (μM)[a] | M.W. | clogP[b] |
|---|---|---|---|---|
| **34** | 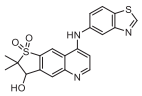 | 2.19 ± 1.57 | 411.5 | 3.65 |
| **35** | 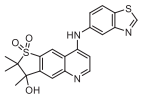 | >20 | 425.5 | 4.23 |
| **36** | 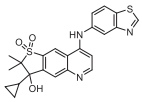 | >20 | 451.6 | 4.72 |
| **37** | 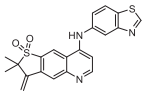 | 1.03 ± 0.10 | 407.5 | 4.81 |
| **38** | 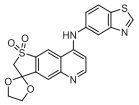 | 0.42 ± 0.08 | 425.5 | 3.49 |
| **39** | 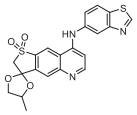 | 1.07 ± 0.40 | 439.5 | 3.86 |
| **47** | 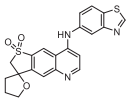 | 3.96 ± 1.81 | 423.5 | 4.06 |
| **61** | 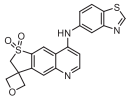 | >20 | 409.5 | 3.54 |
| **1** | | 1.51 ± 0.14 | 383.5 | 4.16 |

[a] Inhibition of TSZ-induced necroptosis in HT-29 cells. [b] Calculated by Molinspiration.

further tested compound **38** in a brief kinase panel (Table 4). Compound **38** showed inhibition of PDGFRa with an $IC_{50}$ = 152 nM,

**Table 4**
Kinase selectivity of compound **38**.

| Kinases | 38 $IC_{50}$ (nM) | Reference $IC_{50}$ (nM) |
|---|---|---|
| EGFR[a] | >10000 | 78 |
| PDGFRa[a] | 152 | 0.58 |
| CDK4/CycD3[a] | >10000 | 43 |
| ALK4[b] | 3737 | 158 |
| BRAF[c] | 1362 | 3.7 |
| m TOR[d] | >10000 | 7.2 |
| PI3Ka[e] | 7770 | 6.0 |

a: Detected by Caliper mobility shift assay and Staurosporine was used as reference compound; b: Detected by ADP-Glo assay with ATP concentration at Km and SB431542 was used as reference; c: Detected by Lantha Screen assay and GW5074 was used as reference; d: Detected by Lance Ultra assay and PI103 was used as reference; e: Detected by ADP-Glo assay with ATP concentration at 25 μM and PI103 was used as reference. These assays were performed by ChemPartner.

while showed moderate or no activity against other kinases. Both compound **38** and GSK′872 displayed significant inhibition of RIPK2 kinase activity at 10 μM concentration (data not shown). RIPK2 is involved in the NOD/RIPK2 signaling pathway and is not related to necroptosis. Collectively, these results demonstrate that compound **38** is a potent necroptosis inhibitor in human and mouse cells, and the inhibition is achieved by suppression of the RIPK3 kinase activity.

### *4.3. Preliminary in vitro safety and DMPK evaluation of lead compound 38*

We were concerned that the ketal functional group presented in compound **38** might impose chemical instability under acidic conditions. We therefore tested compound **38** in simulated gastric fluid (pH 1.2). Compound **38** remained intact after 24 h. We next evaluated compound **38** for its in vitro safety and DMPK profiles. As shown in Table 5, compound **38** exhibited moderate inhibition of CYP1A2 and 2C19 at 10 μM concentration (37% and 20%, respectively), and minimal inhibition of CYP2C9, 2D6, and 3A4. This favorable CYP isozyme inhibition profile suggested low drug/drug interaction liability for compound **38**. A standard patch clamp (express) experiment was used to assess compound **38** for its inhibition of the human ether-a-go-go related gene (hERG) potassium channel. Compound **38** exhibited very low inhibition ($IC_{50}$ > 30 μM) of hERG (positive control: cisapride, 0.03 μM), suggesting low potential cardiotoxicity related to inhibition of hERG. The DMPK profile of compound **38** was summarized in Table 6. Compound **38** was found to be highly bound to plasma proteins cross species (97.1, 98.7, and 97.3%; human, rat, and mouse, respectively). Permeability of compound **38** was measured in a Caco-2 assay. Compound **38** was highly permeable ($35 \times 10^{-6}$ cm/s) with low efflux ratio (0.72), indicating good absorption in the gastrointestinal track. Lastly, compound **38** displayed moderate to high clearance in human (60 mL/min/kg) and mouse (270 mL/min/kg) liver microsomes.

### *4.4. In vivo evaluation of lead compound 38 in the SIRS mouse model*

Necroptosis is involved in many inflammatory disorders. One acute model is the TNFα-induced systemic inflammatory response syndrome (SIRS) [43,44]. Compound **38** was evaluated in the SIRS model for its in vivo *anti*-necroptosis efficacy. C57BL/6 mice were treated with vehicle or compound **38** (5 mg/kg, i.p.) for 15 min prior to intravenous injection of mouse TNFα (0.35 μg/g TNFα per mouse). Treatment of compound **38** strongly reduced TNFα-induced hypothermia and lethal shock in mice (Fig. 6a and b). Moreover, treatment of compound **38** significantly reduced TNFα-induced IL-6 production in serum (Fig. 6c). These results demonstrate that inhibition of RIPK3 by compound **38** provides strong protection against TNF-induced SIRS, highlighting the potential of compound **38** as a lead for the development of anti-inflammatory therapeutics.

## 5. Conclusion

Guided by molecular docking studies based on available RIPK3-small molecule crystal complex, the current structural modification identifies a number of compounds with improved *anti*-necroptosis activity compared with GSK′872, exemplified by compound **38**. Mechanistic studies demonstrate that compound **38** potently binds to RIPK3 ($K_d$ = 7.1 nM) with over 800-fold selectivity over RIPK1 ($K_d$ = 6000 nM). Consistently, compound **38** inhibits RIPK3 kinase function in the ATP-Glo assay without affecting RIPK1 kinase

**Table 5**
Preliminary in vitro safety evaluation of compound **38**.

| Compd. | hERG (μM) | % of CYP inhibiton(10 μM) | | | | | |
|---|---|---|---|---|---|---|---|
| | | 1A2 | 2C9 | 2C19 | 2D6 | CYP3A4 (midazolam) | CYP3A4 (testosterone) |
| **38** | >30 | 37.04 | −6.33 | 19.88 | −5.26 | −13.67 | 9.60 |

**Table 6**
Preliminary in vitro DMPK evaluation of compound **38**.

| Compd. | Protein binding (%) | Caco-2 Permeability | | | Metabolic stability | | | |
|---|---|---|---|---|---|---|---|---|
| | | A-B ($10^{-6}$cm $s^{-1}$) | B-A ($10^{-6}$cm $s^{-1}$) | B-A/A-B | $T_{1/2}$(min) | | $Cl_{int}$(mL/min/kg) | |
| | | | | | HLM[d] | MLM[e] | HLM | MLM |
| **38** | 97.1(H)[a]<br>98.7(R)[b]<br>97.3(M)[c] | 35.24 | 25.33 | 0.72 | 28.75 | 20.26 | 60.47 | 269.40 |

H[a]: human; R[b]: rat; M[c]: mouse; HLM[d]: human liver microsomes; MLM[e]: mouse liver microsomes.

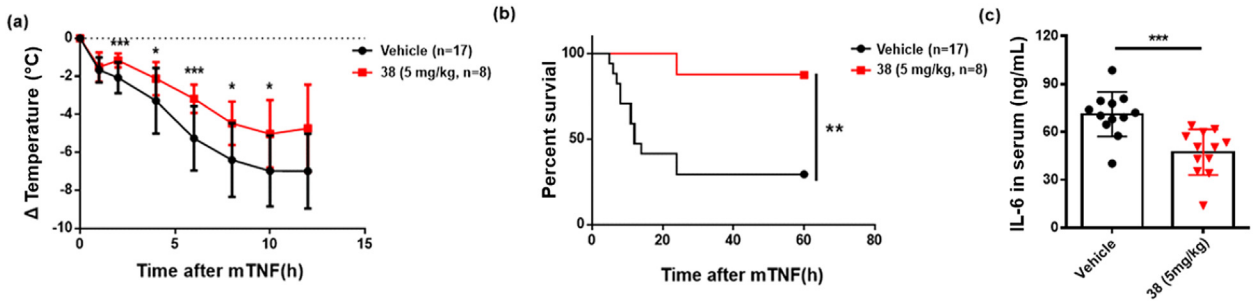


**Fig. 6.** Compound **38** protected mice from SIRS. Body temperature (a), survival curve (b), and serum level of IL-6 (c) of C57BL/6 mice injected with TNFα (0.35 μg/g TNFα) after pretreatment with compound **38** (5 mg/kg).

function. Moreover, compound **38** displays favorable in vitro safety profiles with minimal inhibition of CYP enzymes and hERG. In addition, compound **38** exhibits similar *anti*-necroptosis potency in both mouse and human cells, making it suitable to be studied in preclinical animal efficacy models. Compound **38** ameliorates hypothermia and lethal shock in C57BL/6 mice in the TNFα-induced systemic inflammatory response syndrome model. The promising in vitro and in vivo pharmacological profiles, combined with moderate physicochemical properties and novel scaffold make compound **38** an attractive lead for the development of RIPK3 inhibitors as potential therapeutics.

## 6. Experimental protocols

### 6.1. Chemistry

General reaction progress was monitored by analytical thin layer chromatography performed on silica gel HSGF254 pre-coated plates. Organic solutions were dried over anhydrous $Na_2SO_4$, and the solvents were removed under reduced pressure. Final compounds were purified with silica gel 100–200 mesh for column chromatography. $^1$H NMR were obtained on 400 MHz (Varian) spectrometer, and $^{13}$C NMR were obtained on 151 MHz or 101 MHz (Varian) spectrometer. Chemical shifts were given in ppm using tetramethylsilane as internal standard. Mass spectra were obtained using an Agilent 1100 LC/MSD Trap SL version Mass Spectrometer. HRMS analysis was recorded on an Agilent 6540 UHD Accurate-Mass Q-TOF LC/MS. Values of optical rotation were measured on a Rudolph Automatic Polarimeter A21101. HPLC method: Waters Acquity UPLC, BEH C18 2.1 mm × 50 mm, 1.7 μm particles. Mobile phase A: 5 mM aqueous ammonium acetate. Mobile phase B: MeOH. Temperature: 24 °C. Gradient: 5–40% B over 1 min, 40–70% B over 1 min, 70–95% B over 4 min, then a 1 min hold at 95% B. Flow: 1.2 mL/min. Detection: UV at 214 and 254 nm.

#### 6.1.1. Methyl 5-nitrobenzo[b]thiophene-2-carboxylate (**7**)

To a solution of **6** (64 g, 346 mmol) in DMF (600 mL) was added $K_2CO_3$ (95.5 g, 692 mmol) and methyl 2-mercaptoacetate (34 mL, 381 mmol). The mixture was stirred at room temperature overnight. The reaction was poured into water (3.5 L) and the resulting solid was filtered, washed with water and dried in vacuum to give the desired product **7** (78.5 g, 96%) as a white solid. $^1$H NMR (400 MHz, $CDCl_3$) δ 8.78 (s, 1H), 8.30 (d, $J$ = 8.8 Hz, 1H), 8.19 (s, 1H), 8.00 (d, $J$ = 8.8 Hz, 1H), 3.99 (s, 3H).

#### 6.1.2. 5-nitrobenzo[b]thiophene-2-carboxylic acid (**8**)

To a solution of **7** (78.5 g, 331 mmol) in MeOH (400 mL) and $H_2O$ (400 mL) was added NaOH (53.0 g, 1.3 mol). The mixture was stirred at 70 °C for 4 h. After cooling to room temperature, the solution was poured into water (4 L) and acidified with conc. HCl. The resulting solid was filtered, washed with water, dried in vacuum to give the desired product **8** (72.6 g, 98%) as a white solid. $^1$H NMR (400 MHz, DMSO-$d_6$) δ 8.97 (s, 1H), 8.49–8.19 (m, 3H).

#### 6.1.3. 5-nitrobenzo[b]thiophene (**9**)

To a solution of **8** (65 g, 291 mmol) in quinoline (500 mL) was added copper powder (18.6 g, 291 mmol). The reaction was stirred at 170 °C under $N_2$ atmosphere for 4 h. The solid was removed via filtration and washed with EA (400 mL). Another EA (2 L) was added to the filtrate to dilute the solution and then the solution was

acidified with conc. HCl with an ice bath. The organic layer was separated, washed with 2N HCl (400 mL), saturate $NaHCO_3$ aqueous solution (400 mL), dried over $Na_2SO_4$, filtrated and concentrated. The residue was rinsed with EA (200 mL) and dried in vacuum to give the desired product **9** (48 g, 78%) as a white solid. $^1$H NMR (400 MHz, DMSO-$d_6$) δ 8.84 (s, 1H), 8.29 (d, $J$ = 9.2 Hz, 1H), 8.17 (d, $J$ = 8.8 Hz, 1H), 8.05 (d, $J$ = 5.2 Hz, 1H), 7.72 (d, $J$ = 5.6 Hz, 1H).

*6.1.4. 3-Bromo-5-nitrobenzo[b]thiophene (**10**)*

To a solution of **9** (19.4 g, 108 mmol) in *DMF* (250 mL) was added NBS (21.2 g, 119 mmol). The mixture was stirred at 60 °C under nitrogen atmosphere for 3 h. The solvent was removed in vacuum. The remaining residue was washed with EA (250 mL) and water (250 mL), dried in vacuum to give the desired product **10** (21.0 g, 75%) as a white solid. $^1$H NMR (400 MHz, DMSO-$d_6$) δ8.49 (s, 1H), 8.40 (d, $J$ = 8.8 Hz, 1H), 8.32–8.25 (m, 2H).

*6.1.5. General procedure for the synthesis of **11a-11b***

To a solution of **9**–**10** (1 eq) in DCM (1 mmol/3 mL) with an ice bath was added 85% *m*-CPBA (3 eq). The mixture was stirred at room temperature overnight. The resulting solid was filtered off and the filtrate was quenched with $Na_2SO_3$, washed with saturated $NaHCO_3$ aqueous solution and extracted with DCM. The combined organic phase was dried over $Na_2SO_4$, filtrated and concentrated. The residue was rinsed with EA and dried in vacuum to give the desired product **11a-11b**.

*6.1.5.1. 5-nitrobenzo[b]thiophene 1,1-dioxide (**11a**).* Compound **11a** was obtained as a white solid (1.2 g, 73%). $^1$H NMR (400 MHz, $CDCl_3$) δ 8.43 (d, $J$ = 8.0 Hz, 1H), 8.24 (s, 1H), 7.91 (d, $J$ = 8.0 Hz, 1H), 7.33 (d, $J$ = 7.2 Hz, 1H), 6.93 (d, $J$ = 6.8 Hz, 1H). LCMS (ESI/APCI) $m/z$: 212.9 [M + H] $^+$.

*6.1.5.2. 3-Bromo-5-nitrobenzo[b]thiophene 1,1-dioxide (**11b**).* Compound **11b** was obtained as a white solid (20.8 g, 99%). $^1$H NMR (400 MHz, DMSO-$d_6$) δ8.56 (dd, $J$ = 8.4 Hz, $J$ = 1.2 Hz, 1H), 8.34 (s, 1H), 8.30 (d, $J$ = 8.4 Hz, 1H), 8.20 (d, $J$ = 1.6 Hz, 1H).

*6.1.6. General procedure for the synthesis of **12a-12b***

To a solution of **11a-11b** (1eq) in EtOH (1 mmol/4 mL) and $H_2O$ (1 mmol/2 mL) was added iron powder (5 eq) and $NH_4Cl$ (5 eq). The mixture was stirred at 85 °C for 2 h. The reaction was filtered through diatomaceous earth and the cake was washed with DCM. The resulting filtrate was extracted with DCM. The combined organic phase was dried over $Na_2SO_4$, filtrated and concentrated. The residue was rinsed with EA, dried in vacuum to give the desired product **12a-12b**.

*6.1.6.1. 5-aminobenzo[b]thiophene 1,1-dioxide (**12a**).* Compound **12a** was obtained as a yellow solid (0.8 g, 77%). $^1$H NMR (400 MHz, $CDCl_3$) δ 8.42 (d, $J$ = 8.4 Hz, 1H), 8.22 (s, 1H), 7.90 (d, $J$ = 8.0 Hz, 1H), 7.33 (d, $J$ = 6.8 Hz, 1H), 6.92 (d, $J$ = 6.8 Hz, 1H). LCMS (ESI/APCI) $m/z$: 181.9 [M + H] $^+$.

*6.1.6.2. 5-Amino-3-bromobenzo[b]thiophene 1,1-dioxide (**12b**).* Compound **12b** was obtained as a yellow solid (15 g, 81%). $^1$H NMR (400 MHz, DMSO-$d_6$) δ 7.84 (s, 1H), 7.47 (s, 1H), 6.89–6.59 (m, 2H), 6.44 (s, 2H). LCMS (ESI/APCI) $m/z$: 257.7 [M - H] $^-$.

*6.1.7. General procedure for the synthesis of **13a-13b***

To a solution of **12a-12b** (1 eq) in EtOH (1 mmol/mL) was added 5-(methoxymethylene)-2,2- dimethyl-1,3-dioxane-4,6-dione (1.1 eq). The mixture was stirred at room temperature for 30 min. The resulting solid was collected via filtration, washed with EtOH (1 mmol/mL) and dried in vacuum to give the desired product **13a-13b**.

*6.1.7.1. 5-(((1,1-dioxidobenzo[b]thiophen-5-yl)amino)methylene)-2,2-dimethyl-1,3-dioxane-4,6-dione (**13a**).* Compound **13a** was obtained as a yellow solid (1.4 g, 90%). $^1$H NMR (400 MHz, $CDCl_3$) δ 11.35 (d, $J$ = 13.2 Hz, 1H), 8.66 (d, $J$ = 13.6 Hz, 1H), 7.78 (d, $J$ = 8.0 Hz, 1H), 7.36 (d, $J$ = 8.0 Hz, 1H), 7.26 (s, 1H), 7.23 (d, $J$ = 7.2 Hz, 1H), 6.85 (d, $J$ = 6.8 Hz, 1H), 1.77 (s, 6H). LCMS (ESI/APCI) $m/z$: 333.7 [M - H] $^-$.

*6.1.7.2. 5-(((3-Bromo-1,1-dioxidobenzo[b]thiophen-5-yl)amino) methylene)-2,2-dimethyl-1,3-dioxane–4,6-dione (**13b**).* Compound **13b** was obtained as a yellow solid (18.0 g, 86%). $^1$H NMR (400 MHz, DMSO-$d_6$) δ11.42 (d, $J$ = 12.8 Hz, 1H), 8.68 (d, $J$ = 13.6 Hz, 1H), 8.13 (s, 1H), 7.99 (s, 1H), 7.90 (s, 2H), 1.69 (s, 6H). LCMS (ESI/APCI) $m/z$: 411.5 [M - H] $^-$.

*6.1.8. General procedure for the synthesis of **14a-14b***

The diphenyl ether (1 mmol/10 mL) was added to a round-bottomed flask and the solvent was heated to 240 °C for 5 min. Intermediate **13a-13b** (1 eq) was added dropwise to the solution. The mixture was stirred for 5 min. After cooling to room temperature, the resulting solid was collected via filtration, washed with ether and dried in vacuum to give the desired product **14a-14b**.

*6.1.8.1. 8-hydroxythieno[2,3-g]quinoline 1,1-dioxide (**14a**).* Compound **14a** was obtained as a grey solid (450 mg, 77%). $^1$H NMR (400 MHz, DMSO-$d_6$) δ 12.28 (s, 1H), 8.29 (s, 1H), 8.00 (d, $J$ = 7.2 Hz, 1H), 7.80 (d, $J$ = 6.8 Hz, 1H), 7.69 (s, 1H), 7.56 (d, $J$ = 6.8 Hz, 1H), 6.18 (d, $J$ = 7.2 Hz, 1H). LCMS (ESI/APCI) $m/z$: 233.8 [M + H] $^+$.

*6.1.8.2. 3-Bromo-8-hydroxythieno[2,3-g]quinoline 1,1-dioxide (**14b**).* Compound **14b** was obtained as a grey solid (5.5 g, 41%). $^1$H NMR (400 MHz, DMSO-$d_6$) δ12.31 (s, 1H), 8.35 (s, 1H), 8.25 (s, 1H), 8.08 (d, $J$ = 7.2 Hz, 1H), 7.77 (s, 1H), 6.23 (d, $J$ = 6.8 Hz, 1H). LCMS (ESI/APCI) $m/z$: 311.6 [M + H] $^+$.

*6.1.9. General procedure for the synthesis of **15a-15b***

Intermediate **14a-14b** (1 eq) was added to $POCl_3$ (1 mmol/2 mL) and then the mixture was stirred at reflux for 2 h to afford a light brown solution. After cooling to room temperature, the excess $POCl_3$ was removed in vacuum. The residue was dissolved in EtOH (1 mmol/4 mL) and benzo[*d*]thiazol-5-amine (1.1 eq) was added subsequently. The mixture was stirred at reflux for 1 h. After cooling to room temperature. The resulting solid was collected via filtration, washed with EtOH and dried in vacuum to give the desired product **15a-15b**.

*6.1.9.1. 8-(benzo[d]thiazol-5-ylamino)thieno[2,3-g]quinoline 1,1-dioxide (**15a**).* Compound **15a** was obtained as a hydrochloride salt (165 mg, 24%). $^1$H NMR (400 MHz, DMSO-$d_6$) δ 14.79 (br s, 1H), 11.15 (s, 1H), 9.54 (s, 1H), 9.31 (s, 1H), 8.56 (d, $J$ = 7.2 Hz, 1H), 8.39 (d, $J$ = 8.4 Hz, 1H), 8.22 (s, 1H), 8.16 (s, 1H), 8.00 (d, $J$ = 7.6 Hz, 1H), 7.81 (d, $J$ = 6.8 Hz, 1H), 7.61 (d, $J$ = 8.4 Hz, 1H), 7.00 (d, $J$ = 6.8 Hz, 1H). LCMS (ESI/APCI) $m/z$: 365.7 [M + H] $^+$.

*6.1.9.2. 8-(benzo[d]thiazol-5-ylamino)-3-bromothieno[2,3-g]quinoline 1,1-dioxide (**15b**).* Compound **15b** was obtained as a hydrochloride salt (6.0 g, 77%). $^1$H NMR (400 MHz, DMSO-$d_6$) δ 11.37 (s, 1H), 9.55 (s, 1H), 9.43 (s, 1H), 8.63 (d, $J$ = 6.8 Hz, 1H), 8.50 (s, 1H), 8.40 (d, $J$ = 8.8 Hz, 1H), 8.27–8.21 (m, 2H), 7.62 (d, $J$ = 8.8 Hz, 1H), 7.04 (d, $J$ = 7.2 Hz, 1H). LC-MS (ESI/APCI) $m/z$: 443.5 [M + H] $^+$.

*6.1.10. 8-(benzo[d]thiazol-5-ylamino)-2,3-dihydrothieno[2,3-g] quinoline 1,1-dioxide (**16**)*

To a solution of **15a** (120 mg, 0.30 mmol) in MeOH (15 mL) was added Pd/C (20 mg). the reaction was stirred at room temperature under hydrogen atmosphere overnight. The solid was removed via filtration. The filtrate was concentrated and purified by silica gel column chromatography (DCM/MeOH = 80/1) to give the desired product **16** (40 mg, 36%) as a white solid. $^1$H NMR (400 MHz, DMSO-$d_6$) δ 9.57 (s, 1H), 9.45 (s, 1H), 9.00 (s, 1H), 8.57 (d, $J$ = 5.6 Hz, 1H), 8.22 (d, $J$ = 8.8 Hz, 1H), 8.06 (s, 1H), 7.98 (s, 1H), 7.56 (d, $J$ = 8.4 Hz, 1H), 7.05 (d, $J$ = 5.2 Hz, 1H), 3.72 (t, $J$ = 6.8 Hz, 2H), 3.54 (t, $J$ = 6.4 Hz, 2H). HRMS (ESI) calcd for $C_{18}H_{13}N_3O_2S_2$, [M + H] $^+$, 368.0522, found, 368.0522. Purity: 94.5%.

*6.1.11. 8-(benzo[d]thiazol-5-ylamino)-3-methoxythieno[2,3-g] quinoline 1,1-dioxide (**17**)*

To a solution of **15b** (300 mg, 0.63 mmol) in MeOH (300 mL) was added $Cs_2CO_3$ (462 mg, 1.42 mmol). The mixture was stirred at room temperature for 20 h the solvent was concentrated and purified by silica gel column chromatography (DCM/MeOH = 100/1) to give the desired product **17** (105 mg, 42%) as a yellow solid. $^1$H NMR (400 MHz, DMSO-$d_6$) δ 9.55 (s, 1H), 9.45 (s, 1H), 9.02 (s, 1H), 8.57 (d, $J$ = 4.8 Hz, 1H), 8.23 (d, $J$ = 8.4 Hz, 1H), 8.06 (s, 1H), 7.92 (s, 1H), 7.55 (d, $J$ = 8.8 Hz, 1H), 7.10 (d, $J$ = 4.8 Hz, 1H), 6.91 (s, 1H), 4.04 (s, 3H). LC-MS (ESI/APCI) $m/z$: 395.7 [M + H] $^+$.

*6.1.12. 8-(benzo[d]thiazol-5-ylamino) thieno[2,3-g] quinolin-3(2H)-one 1,1-dioxide (**18**)*

To a solution of **17** (15 mg, 0.04 mmol) in $CH_3CN$ (2 mL) was added conc. HCl (0.5 mL). The mixture was stirred at 80 °C overnight. The reaction was poured into water (20 mL). The resulting solid was collected via filtration, washed with IPA (5 mL) and dried in vacuum to give the desired product **18** (12 mg, 83%) as a hydrochloride salt. $^1$H NMR (400 MHz, DMSO-$d_6$) δ 14.97 (s, 1H), 11.64 (s, 0.67H), 11.30 (s, 0.33H), 9.70 (s, 0.67H), 9.55 (s, 1H), 9.30 (s, 0.33H), 8.72 (d, $J$ = 6.4 Hz, 0.67H), 8.63 (s, 0.67H), 8.59 (d, $J$ = 4.8 Hz, 0.33H), 8.43 (d, $J$ = 8.8 Hz, 1H), 8.28 (s, 0.67H), 8.24 (s, 0.33H), 8.20 (s, 0.33H), 7.70–7.58 (m, 1H), 7.07 (d, $J$ = 6.4 Hz, 0.67H), 7.00 (d, $J$ = 4.4 Hz, 0.33H), 6.58 (s, 0.33H), 4.85 (s, 1.33H). HRMS (ESI) calcd for $C_{18}H_{11}N_3O_3S_2$, [M + H] $^+$, 382.0315, found, 382.0314. Purity: 95.4%.

*6.1.13. General procedure for the synthesis of **20a-20c***

To a solution of **19** (1 eq) in DMSO (1 mmol/2.5 mL) was added sodium ethyl sulfonate (1 eq). The mixture was stirred at room temperature overnight. NaH (1 eq) was added slowly with an ice bath. Recovering to room temperature. the mixture was stirred for 3 h. Halogenated hydrocarbon (3 eq) was added and the reaction was stirred for another 5 h. EA (1 mmol/15 mL) was added to dilute the solution and the reaction was acidified with 1 N HCl to adjust pH to 5. The organic layer was separated, dried with $Na_2SO_4$, filtrated and concentrated. The residue was purified by silica gel column chromatography (PE/EA = 10/1) to give the desired product **20a-20c**.

*6.1.13.1. 2,2-Dimethyl-5-nitrobenzo[b]thiophen-3(2H)-one 1,1-dioxide (**20a**).* Compound **20a** was obtained as a yellow solid (11 g, 43%)。 $^1$H NMR (400 MHz, DMSO-$d_6$) δ 8.83 (d, $J$ = 8.0 Hz, 1H), 8.62 (s, 1H), 8.52 (d, $J$ = 8.8 Hz, 1H), 1.56 (s, 6H). LCMS (ESI/APCI) $m/z$: 277.7 [M + Na] $^+$.

*6.1.13.2. 2-Ethyl-2-methyl-5-nitrobenzo[b]thiophen-3(2H)-one 1,1-dioxide (**20b**).* Compound **20b** was obtained (2.4 g, 45%) as a grey solid. $^1$H NMR (400 MHz, $CDCl_3$) δ8.80 (s, 1H),8.75 (d, $J$ = 8.4 Hz, 1H), 8.22 (d, $J$ = 8.4 Hz, 1H), 2.26–1.95 (m, 2H), 1.64 (s, 3H), 1.10 (t, $J$ = 7.2 Hz, 3H). LCMS (ESI/APCI) $m/z$: 268.8 [M - H] $^-$.

*6.1.13.3. 2-(cyclopropylmethyl)-2-methyl-5-nitrobenzo[b]thiophen-3(2H)-one 1,1-dioxide (**20c**).* Compound **20c** was obtained as a yellow oil (400 mg, 6.8%).$^1$H NMR (400 MHz, $CDCl_3$) δ8.80 (s, 1H), 8.75 (d, $J$ = 8.0 Hz, 1H), 8.22 (d, $J$ = 8.0 Hz, 1H), 2.18–2.05 (m, 1H), 1.95–1.85 (m, 1H), 1.71 (s, 3H), 0.92–0.77 (m, 1H), 0.60–0.48 (m, 1H), 0.45–0.35 (m, 1H), 0.16–0.14 (m, 2H). LCMS (ESI/APCI) $m/z$: 295.8 [M + H] $^+$.

*6.1.14. General procedure for the synthesis of **21a-21c***

To a solution of **20a-20c** (1.0 eq) in EtOH (1 mmol/10 mL) and $H_2O$ (1 mml/1.5 mL) was added iron powder (5 eq) and $NH_4Cl$ (5 eq). The mixture was stirred at 85 °C for 2 h. The reaction was filtered through diatomaceous earth and the cake was washed with DCM (1 mmol/50 mL). The resulting filtrate was washed with saturated $NaHCO_3$ aqueous solution, dried over $Na_2SO_4$, filtrated and concentrated. The residue was rinsed with EA, dried in vacuum to give the desired product **21a-21c**.

*6.1.14.1. 5-Amino-2,2-dimethylbenzo[b]thiophen-3(2H)-one 1,1-dioxide (**21a**).* Compound **21a** was obtained as a yellow solid (8.7 g, 90%). $^1$H NMR (400 MHz, $CDCl_3$) δ 7.75 (d, $J$ = 8.4 Hz, 1H), 7.12–7.07 (m, 1H), 7.07–7.05 (m, 1H), 4.77 (br s, 2H), 1.58 (s, 6H). LCMS (ESI/APCI) $m/z$: 225.9 [M + H] $^+$

*6.1.14.2. 5-Amino-2-ethyl-2-methylbenzo[b]thiophen-3(2H)-one 1,1-dioxide (**21b**).* Compound **21b** was obtained as a yellow solid (700 mg, 60%). $^1$H NMR (400 MHz, $CDCl_3$) δ7.74 (d, $J$ = 8.0 Hz, 1H), 7.10–7.00 (m, 2H), 4.38 (s, 2H), 2.20–1.98 (m, 2H), 1.56 (s, 3H), 1.06 (t, $J$ = 7.2 Hz, 3H). LCMS (ESI/APCI) $m/z$: 239.9 [M + H] $^+$.

*6.1.14.3. 5-Amino-2-(cyclopropylmethyl)-2-methylbenzo[b]thiophen-3(2H)-one 1,1-dioxide (**21c**).* Compound **21c** was obtained as a yellow oil (240 mg, 66%). $^1$H NMR (400 MHz, $CDCl_3$) δ7.75 (d, $J$ = 8.4 Hz, 1H), 7.14–7.00 (m, 2H), 4.37 (s, 2H), 2.10–1.98 (m, 1H), 1.90–1.80 (m, 1H), 1.64 (s, 3H), 1.10–0.80 (m, 1H), 0.65–0.35 (m, 2H), 0.16–0.05 (m, 2H). LCMS (ESI/APCI) $m/z$: 265.8 [M + H] $^+$.

*6.1.15. General procedure for the synthesis of **22a-22c***

To a solution of **21a-21c** (1 eq) in MeOH (1 mmol/4 mL) and $H_2O$ (1 mmol/2 mL) was added Oxone (1 eq). Then NaBr (1 eq) dissolved in $H_2O$ (1 mmol/mL) was added dropwise. The mixture was stirred at room temperature for 4 h. Saturated $NaHCO_3$ (1 mmol/10 mL) aqueous solution was added to quench the reaction. The aqueous layer was extracted with DCM (1 mmol/10 mL * 3). The combined organic phase was dried over $Na_2SO_4$, filtrated and concentrated. The residue was purified by silica gel column chromatography (DCM/MeOH = 50/1) to give the desired product **22a-22c**.

*6.1.15.1. 5-Amino-4-bromo-2,2-dimethylbenzo[b]thiophen-3(2H)-one 1,1-dioxide (**22a**).* Compound **22a** was obtained as a yellow solid (10 g, 85%). $^1$H NMR (400 MHz, DMSO-$d_6$) δ 7.82 (d, $J$ = 8.8 Hz, 1H), 7.31 (d, $J$ = 8.4 Hz, 1H), 6.74 (br s, 2H), 1.45 (s, 6H). LCMS (ESI/APCI) $m/z$: 303.6 [M + H] $^+$.

*6.1.15.2. 5-Amino-4-bromo-2-ethyl-2-methylbenzo[b]thiophen-3(2H)-one 1,1-dioxide (**22b**).* Compound **22b** was obtained as a yellow solid (500 mg, 66%). $^1$H NMR (400 MHz, DMSO-$d_6$) δ 7.80 (d, $J$ = 8.4 Hz, 1H), 7.30 (d, $J$ = 8.4 Hz, 1H), 6.73 (br s, 2H), 1.96–1.86 (m, 2H), 1.43 (s, 3H), 0.92 (t, $J$ = 7.2 Hz, 3H).

*6.1.15.3. 5-Amino-4-bromo-2-(cyclopropylmethyl)-2-methylbenzo[b] thiophen-3(2H)-one 1,1-dioxide (**22c**).* Compound **22c** was obtained as a yellow oil (211 mg, 83%). $^1$H NMR (400 MHz, $CDCl_3$) δ 7.72 (d,

$J = 7.6$ Hz, 1H), 7.15 (d, $J = 8.0$ Hz, 1H), 4.94 (s, 2H), 2.10–1.98 (m, 1H), 1.90–1.75 (m, 1H), 1.58 (s, 3H), 0.90–0.85 (m, 1H), 0.55–0.35 (m, 2H), 0.16–0.05 (m, 2H). LCMS (ESI/APCI) *m/z*: 343.7 [M + H] $^+$.

*6.1.16. General procedure for the synthesis of **23a-23c***

To a solution of **22a-22c** (1 eq) in EtOH (1 mmol/2 mL) was added 5-(methoxymethylene)-2,2-dimethyl-1,3-dioxane-4,6-dione (1.1 eq). The mixture was stirred at room temperature for 30 min. The resulting solid was collected via filtration, washed with EtOH (1 mmol/1 mL) and dried in vacuum to give the desired product **23a-23c**.

*6.1.16.1. 5-(((4-Bromo-2,2-dimethyl-1,1-dioxido-3-oxo-2,3-dihydrobenzo[b]thiophen-5-yl) amino) methylene)-2,2-dimethyl-1,3-dioxane-4,6-dione (**23a**).* Compound **23a** was obtained as a white solid (13 g, 86%). $^1$H NMR (400 MHz, DMSO-$d_6$) δ 11.84 (d, $J = 13.6$ Hz, 1H), 8.92 (d, $J = 13.6$ Hz, 1H), 8.54 (d, $J = 8.4$ Hz, 1H), 8.31 (d, $J = 8.8$ Hz, 1H), 1.71 (s, 6H), 1.53 (s, 6H).

*6.1.16.2. 5-(((4-Bromo-2-ethyl-2-methyl-1,1-dioxido-3-oxo-2,3-dihydrobenzo[b]thiophen-5-yl)amino) methylene)-2,2-dimethyl-1,3-dioxane-4,6-dione (**23b**).* Compound **23b** was obtained as a white solid (673 mg, 90%). $^1$H NMR (400 MHz, DMSO-$d_6$) δ 11.83 (d, $J = 13.6$ Hz, 1H), 8.91 (d, $J = 13.2$ Hz, 1H), 8.52 (d, $J = 8.8$ Hz, 1H), 8.29 (d, $J = 8.8$ Hz, 1H), 2.03–1.94 (m, 2H), 1.71 (s, 6H), 1.51 (s, 3H), 0.96 (t, $J = 7.2$ Hz, 3H). LCMS (ESI/APCI) *m/z*: 469.6 [M - H] $^-$.

*6.1.16.3. 5-(((4-Bromo-2-(cyclopropylmethyl)-2-methyl-1,1-dioxido-3-oxo-2,3-dihydrobenzo[b].*
thiophen-5-yl)amino)methylene)-2,2-dimethyl-1,3-dioxane-4,6-dione (**23c**).

Compound **23c** was obtained as a white solid (290 mg, 93%). $^1$H NMR (400 MHz, DMSO-$d_6$) δ 11.82 (d, $J = 11.6$ Hz, 1H), 8.90 (d, $J = 12.8$ Hz, 1H), 8.51 (d, $J = 8.0$ Hz, 1H), 8.29 (d, $J = 8.4$ Hz, 1H), 2.04–1.98 (m, 1H), 1.83–1.77 (m, 1H), 1.71 (s, 6H), 1.57 (s, 3H), 0.69–0.62 (m, 1H), 0.44–0.38 (m, 1H), 0.31–0.25 (m, 1H), 0.05 (d, $J = 4.4$ Hz, 2H). LCMS (ESI/APCI) *m/z*: 495.5 [M - H] $^-$.

*6.1.17. General procedure for the synthesis of **24a-24c***

The diphenyl ether (1 mmol/10 mL) was added to a round-bottomed flask and the solvent was heated to 240 °C for 5 min. Intermediate **23a-23c** (1 eq) was added dropwise to the solution. The mixture was stirred for 5 min. After cooling down to room temperature, the resulting solid was collected via filtration, washed with ether (5 mL) and dried in vacuum to give the desired product **24a-24c**.

*6.1.17.1. 4-Bromo-8-hydroxy-2,2-dimethylthieno[2,3-g]quinolin-3(2H)-one 1,1-dioxide (**24a**).* Compound **24a** was obtained as a grey solid (6.0 g, 60%).$^1$H NMR (400 MHz, DMSO-$d_6$) δ 11.78 (s, 1H), 8.60 (s, 1H), 8.06 (s, 1H), 6.34 (d, $J = 7.2$ Hz, 1H), 1.54 (s, 6H). LCMS (ESI/APCI) *m/z*: 353.6 [M - H] $^-$.

*6.1.17.2. 4-Bromo-2-ethyl-8-hydroxy-2-methylthieno[2,3-g]quinolin-3(2H)-one 1,1-dioxide (**24b**).* Compound **24b** was obtained as a brown solid (100 mg, 19%). $^1$H NMR (400 MHz, DMSO-$d_6$) δ11.77 (s, 1H), 8.59 (s, 1H), 8.05 (s, 1H), 6.35 (s, 1H), 2.10–1.98 (m, 2H), 1.53 (s, 3H), 0.96 (t, $J = 7.2$ Hz, 3H). LCMS (ESI/APCI) *m/z*: 369.7 [M + H] $^+$.

*6.1.17.3. 4-Bromo-2-(cyclopropylmethyl)-8-hydroxy-2-methylthieno [2,3-g]quinolin-3(2H)-one 1,1-dioxide (**24c**).* Compound **24c** was obtained as a white solid (60 mg, 26%). $^1$H NMR (400 MHz, DMSO-$d_6$) δ 11.78 (s, 1H), 8.59 (s, 1H), 8.09–8.01 (m, 1H), 8.34 (d, $J = 7.2$ Hz, 1H), 2.01–1.95 (m, 1H), 1.88–1.81 (m, 1H), 1.59 (s, 3H), 0.73–0.63 (m, 1H), 0.42–0.37 (m, 1H), 0.30–0.24 (m, 1H), 0.04 (d, $J = 3.2$ Hz, 2H). LCMS (ESI/APCI) *m/z*: 395.6 [M + H] $^+$.

*6.1.18. General procedure for the synthesis of **25a-25c***

To a solution of **24a-24c** (1 eq) in IPA (1 mmol/50 mL) and $H_2O$ (1 mmol/5 mL) was added 10% Pd/C (1 mmol/50 mg) and $Et_3N$ (1 mmol/3 mL). The reaction was stirred under $H_2$ atmosphere for 1.5 h. Saturated $Na_2SO_3$ (1 mmol/50 mL) aqueous solution and DCM (1 mmol/100 mL) were added. The organic layer was separated, dried over $Na_2SO_4$, filtrated and concentrated to give the desired product **25a-25c**.

*6.1.18.1. 8-Hydroxy-2,2-dimethylthieno[2,3-g]quinolin-3(2H)-one 1,1-dioxide (**25a**).* Compound **25a** was obtained as a yellow solid (4.0 g, 86%). $^1$H NMR (400 MHz, DMSO-$d_6$) δ 12.42 (s, 1H), 8.62 (s, 1H), 8.20–8.10 (m, 2H), 6.26 (d, $J = 7.2$ Hz, 1H), 1.53 (s, 6H). LCMS (ESI/APCI) *m/z*: 277.8 [M + H] $^+$.

*6.1.18.2. 2-Ethyl-8-hydroxy-2-methylthieno[2,3-g]quinolin-3(2H)-one 1,1-dioxide (**25b**).* Compound **25b** was obtained as a grey solid (50 mg, 61%)。 $^1$H NMR (400 MHz, DMSO-$d_6$) δ12.41 (br s, 1H), 8.62 (s, 1H), 8.22–8.10 (m, 2H), 6.27 (d, $J = 7.6$ Hz, 1H), 2.10–1.90 (m, 2H), 1.51 (s, 3H), 0.97 (t, $J = 7.6$ Hz, 3H). LCMS (ESI/APCI) *m/z*: 291.7 [M + H] $^+$.

*6.1.18.3. 2-(cyclopropylmethyl)-8-hydroxy-2-methylthieno[2,3-g] quinolin-3(2H)-one 1,1-dioxide (**25c**).* Compound **25c** was obtained as a yellow solid (50 mg, 61%). $^1$H NMR (400 MHz, DMSO-$d_6$) δ12.41 (s, 1H), 8.62 (s, 1H), 8.16 (s, 1H), 8.08–8.04 (m, 1H), 6.27 (d, $J = 7.6$ Hz, 1H), 2.04–1.95 (m, 1H), 1.96–1.80 (m, 1H), 1.59 (s, 3H), 0.80–0.70 (m, 1H), 0.44–0.38 (m, 1H), 0.34–0.28 (m, 1H), 0.12–0.05 (m, 2H). LCMS (ESI/APCI) *m/z*: 315.7 [M - H] $^-$.

*6.1.19. General procedure for the synthesis of **26–33***

Intermediate **25a-25c** (1 eq) was added to $POCl_3$ (1 mmol/4 mL) and then the mixture was stirred at reflux for 2 h to afford a light brown solution. After cooling to room temperature, the excess $POCl_3$ was removed in vacuum. The residue was dissolved in EtOH (1 mmol/10 mL) and subsequently various aromatic amine (1.1 eq) was added. The mixture was stirred at reflux for 1 h. After cooling to room temperature. The resulting solid was collected via filtration, washed with EtOH and dried in vacuum to give the desired product **26–33**.

*6.1.19.1. 8-(benzo[d]thiazol-5-ylamino)-2,2-dimethylthieno[2,3-g] quinolin-3(2H)-one 1,1-dioxide (**26**).* Compound **26** was obtained as a yellow solid (450 mg, 50%)。 $^1$H NMR (400 MHz, DMSO-$d_6$) δ 11.39 (s, 1H), 9.71 (s, 1H), 9.55 (s, 1H), 8.73 (d, $J = 6.8$ Hz, 1H), 8.63 (s, 1H), 8.41 (d, $J = 8.4$ Hz, 1H), 8.25 (s, 1H), 7.64 (d, $J = 7.6$ Hz, 1H), 7.10 (d, $J = 6.8$ Hz, 1H), 1.61 (s, 6H). $^{13}$C NMR (151 MHz, DMSO-$d_6$) δ 194.4, 157.6, 154.8, 154.1, 150.5, 149.3, 138.0, 137.0, 129.9, 129.3, 127.0, 124.5, 123.4, 121.6, 118.9, 116.8, 103.7, 64.1, 40.1, 39.9, 39.8, 39.7, 39.5, 39.4, 39.2, 39.1, 19.5. HRMS (ESI) calcd for $C_{20}H_{15}N_3O_3S_2$, [M + H] $^+$, 410.0628, found, 410.0628. Purity: 95.0%.

*6.1.19.2. 8-(benzo[d]thiazol-5-ylamino)-2-ethyl-2-methylthieno[2,3-g]quinolin-3(2H)-one 1,1-dioxide (**27**).* Compound **27** was obtained as a yellow solid (15 mg, 30%)。 $^1$H NMR (400 MHz, DMSO-$d_6$) δ 11.46 (s, 1H), 9.72 (s, 1H), 9.55 (s, 1H), 8.72 (s, 1H), 8.66 (s, 1H), 8.41 (d, $J = 8.4$ Hz, 1H), 8.25 (s, 1H), 7.64 (d, $J = 8.0$Hz, 1H), 7.09 (d, $J = 6.4$ Hz, 1H), 2.20–1.99 (m, 2H), 1.59 (s, 3H), 1.02 (t, $J = 7.6$ Hz, 3H). $^{13}$C NMR (151 MHz, DMSO-$d_6$) δ 193.5, 158.5, 155.4, 153.9, 146.1, 141.6, 139.1, 135.2, 133.0, 132.0, 124.1, 122.7, 122.4, 120.4, 119.4, 118.5, 102.2, 68.0, 26.8, 16.2, 8.3. HRMS (ESI) calcd for $C_{21}H_{17}N_3O_3S_2$, [M + H] $^+$, 424.0784, found, 424.0785. Purity: 96.3%.

*6.1.20. 3.8-(benzo[d]thiazol-5-ylamino)-2-(cyclopropylmethyl)-2-methylthieno[2,3-g]quinolin-3(2H)-one 1,1-dioxide (**28**)*

Compound **28** was obtained as a yellow solid (12 mg, 44%)。$^1$H NMR (400 MHz, DMSO-$d_6$) δ 11.33 (s, 1H), 9.69 (s, 1H), 9.55 (s, 1H), 8.72 (d, $J$ = 6.8 Hz, 1H), 8.59 (s, 1H), 8.41 (d, $J$ = 8.4 Hz, 1H), 8.24 (s, 1H), 7.63 (d, $J$ = 8.4 Hz, 1H), 7.11 (d, $J$ = 6.4 Hz, 1H), 2.15–2.07 (m, 1H), 1.96–1.85 (m, 1H), 1.66 (s, 3H), 0.82–0.70 (m, 1H), 0.50–0.40 (m, 1H), 0.34–0.26 (m, 1H), 0.20–0.05 (m, 2H). $^{13}$C NMR (151 MHz, DMSO-$d_6$) δ 194.3, 157.6, 154.5, 154.1, 150.3, 149.5, 138.0, 137.4, 130.2, 129.9, 126.3, 124.3, 123.4, 121.6, 118.6, 116.9, 103.6, 68.2, 16.8, 6.2, 5.1, 4.78. HRMS (ESI) calcd for $C_{23}H_{19}N_3O_3S_2$, [M + H] $^+$, 450.0941, found, 450.0942. Purity: 99.1%.

*6.1.20.1. 8-((5-Fluoro-1H-indazol-3-yl)amino)-2,2-dimethylthieno[2,3-g]quinolin-3(2H)-one 1,1-dioxide (**29**).* Compound **29** was obtained as a brown solid (20 mg, 16%). $^1$H NMR (400 MHz, DMSO-$d_6$) δ 12.99 (s, 1H), 9.86 (s, 1H), 9.65 (s, 1H), 8.81 (d, $J$ = 5.2 Hz, 1H), 8.48 (s, 1H), 7.82 (d, $J$ = 5.2 Hz, 1H), 7.77 (d, $J$ = 8.8 Hz, 1H), 7.60 (dd, $J$ = 4.0Hz, 8.8 Hz, 1H),7.34 (t, $J$ = 8.4 Hz, 1H), 1.59 (s, 6H). $^{13}$C NMR (101 MHz, DMSO-$d_6$) δ 194.5, 156.56 (d, $J$ = 235.0 Hz), 155.0, 150.2, 147.7, 141.6 (d, $J$ = 5.7 Hz), 138.0, 137.1, 129.2, 127.1, 124.1, 119.2, 116.6 (d, $J$ = 27.6 Hz), 115.5 (d, $J$ = 10.5 Hz), 112.1 (d, $J$ = 9.5 Hz), 105.7, 104.4 (d, $J$ = 24.8 Hz), 64.1, 19.6. HRMS (ESI) calcd for $C_{20}H_{15}FN_4O_3S$, [M + H] $^+$, 411.0922, found, 411.0922. Purity: 98.0%.

*6.1.20.2. 8-((3,4-Dimethyl-1H-pyrazol-5-yl)amino)-2,2-dimethylthieno[2,3-g]quinolin-3(2H)-one 1,1-dioxide (**30**).* Compound **30** was obtained as a yellow solid (16 mg, 22%). $^1$H NMR (400 MHz, DMSO-$d_6$) δ 12.35 (s, 1H), 9.47 (s, 1H), 9.32 (s, 1H), 8.64 (d, $J$ = 4.8 Hz, 1H), 8.40 (s, 1H), 6.92 (d, $J$ = 5.2 Hz, 1H), 2.21 (s, 3H), 1.84 (s, 3H), 1.56 (s, 6H). $^{13}$C NMR (151 MHz, DMSO-$d_6$) δ 194.5, 154.6, 150.3, 149.9, 145.7, 137.1, 136.8, 129.1, 126.9, 123.6, 119.0, 105.7, 104.2, 64.1, 19.6, 9.6, 7.1. HRMS (ESI) calcd for $C_{18}H_{18}N_4O_3S$, [M + H] $^+$, 371.1172, found, 371.1173. Purity: 95.5%.

*6.1.20.3. 8-((5-Hydroxy-2-methylphenyl)amino)-2,2-dimethylthieno[2,3-g]quinolin-3(2H)-one 1,1-dioxide (**31**).* Compound **31** was obtained as a yellow solid (15 mg, 20%). $^1$H NMR (400 MHz, DMSO-$d_6$) δ 9.49 (s, 1H), 9.41 (s, 1H), 9.33 (s, 1H), 8.60 (d, $J$ = 4.4 Hz, 1H), 8.40 (s, 1H), 7.19 (d, $J$ = 8.0 Hz, 1H), 6.77–6.66 (m, 2H), 6.34 (d, $J$ = 4.0 Hz, 1H), 2.05 (s, 3H), 1.57 (s, 6H). $^{13}$C NMR (101 MHz, DMSO-$d_6$) δ 194.6, 156.5, 154.6, 150.5, 150.4, 137.6, 136.7, 132.1, 129.3, 126.9, 124.5, 123.8, 119.0, 114.5, 113.6, 103.2, 64.2, 55.0, 19.6, 16.7. HRMS (ESI) calcd for $C_{20}H_{18}N_2O_4S$, [M + H] $^+$, 383.1060, found, 383.1060. Purity: 91.1%.

*6.1.20.4. 8-((2-Fluoro-5-hydroxyphenyl)amino)-2,2-dimethylthieno[2,3-g]quinolin-3(2H)-one 1,1-dioxide (**32**).* Compound **32** was obtained as a white solid (25 mg, 29%). $^1$H NMR (400 MHz, DMSO-$d_6$) δ 11.13 (s, 1H), 9.98 (s, 1H), 9.67 (s, 1H), 8.79 (d, $J$ = 6.4 Hz, 1H), 8.64 (s, 1H), 7.33 (t, $J$ = 9.6 Hz, 1H), 7.00–6.85 (m, 2H), 6.78 (d, $J$ = 4.0 Hz, 1H), 1.60 (s, 6H). $^{13}$C NMR (101 MHz, DMSO-$d_6$) δ 193.8, 155.5, 154.7 (d, $J$ = 1.3 Hz), 149.7 (d, $J$ = 239.5 Hz), 146.3, 141.3, 139.0, 131.9, 124.1 (d, $J$ = 13.8 Hz), 122.0, 120.6, 118.8, 117.6 (d, $J$ = 20.7 Hz), 116.5 (d, $J$ = 7.0 Hz), 113.8, 102.8, 64.6, 19.5. HRMS (ESI) calcd for $C_{19}H_{15}FN_2O_4S$, [M + H] $^+$, 387.0809, found, 387.0809. Purity: 97.5%.

*6.1.20.5. 8-((2,4-Difluoro-5-hydroxyphenyl)amino)-2,2-dimethylthieno[2,3-g]quinolin-3(2H)-one 1,1-dioxide (**33**).* Compound **33** was obtained as a yellow solid (10 mg, 14%). $^1$H NMR (400 MHz, DMSO-$d_6$) δ 10.16 (s, 1H), 9.47 (s, 1H), 9.35 (s, 1H), 8.69 (s, 1H), 8.44 (s, 1H), 7.45 (t, $J$ = 10.4 Hz, 1H), 7.03 (t, $J$ = 8.0 Hz, 1H), 6.61 (s, 1H), 1.57 (s, 6H). $^{13}$C NMR (151 MHz, DMSO-$d_6$) δ 194.5, 154.6, 150.2, 149.7, 149.5 (dd, $J$ = 29.4, 10.8 Hz), 147.9 (dd, $J$ = 29.4, 10.8 Hz), 142.1 (d, $J$ = 11.4 Hz), 137.0, 129.3, 127.0, 123.8, 122.0 (d, $J$ = 13.2 Hz), 118.9, 115.4, 105.8 (t, $J$ = 24.2 Hz), 103.9, 64.2, 19.5. HRMS (ESI) calcd for $C_{19}H_{14}F_2N_2O_4S$, [M + H] $^+$, 405.0715, found, 405.0716. Purity: 95.0%.

*6.1.21. 8-(benzo[d]thiazol-5-ylamino)-3-hydroxy-2,2-dimethyl-2,3-dihydrothieno[2,3-g] quinoline 1,1-dioxide (**34**)*

To a solution of **26** (50 mg, 0.11 mmol) in MeOH (3 mL) and DCM (5 mL) was added $NaBH_4$ (11 mg, 0.11 mmol). The reaction was stirred at room temperature for 30 min. Saturated $NH_4Cl$ (1 mL) aqueous solution was added to quench the reaction. The reaction was concentrated and purified by silica gel column chromatography (DCM/MeOH = 20/1) to give the desired product **34** (8 mg, 16%) as a yellow solid. $^1$H NMR (400 MHz, DMSO-$d_6$) δ 9.61 (s, 1H), 9.45 (s, 1H), 9.04 (s, 1H), 8.58 (s, 1H), 8.23 (d, $J$ = 8.4 Hz,1H), 8.07 (s, 1H), 8.02 (s, 1H), 7.56 (d, $J$ = 8.0 Hz, 1H), 7.07 (s, 1H), 6.66 (d, $J$ = 6.0 Hz, 1H), 5.12 (d, $J$ = 5.6 Hz, 1H),1.50 (s, 3H), 1.17 (s, 3H). $^{13}$C NMR (101 MHz, DMSO-$d_6$) δ 157.5, 154.2, 153.4, 151.1, 149.1, 140.1, 138.5, 133.0, 129.4, 126.1, 123.2, 121.5, 119.6, 117.8, 116.4, 102.1, 73.9, 65.6, 17.6, 16.6. HRMS (ESI) calcd for $C_{20}H_{17}N_3O_3S_2$, [M + H] $^+$, 412.0784, found, 412.0793. Purity: 98.4%

*6.1.22. General procedure for the synthesis of **35**–**36***

To a solution of **26** (1 eq) in THF (5 mL) under $N_2$ atmosphere was added Grignard reagent (3 eq) with an ice bath. The mixture was stirred at room temperature for 1 h $H_2O$ was added to quench the reaction. The aqueous layer was extracted with DCM (1 mmol/30 mL * 3). The combined organic layer was dried over $Na_2SO_4$, filtrated and concentrated. The residue was purified by silica gel column chromatography (DCM/MeOH = 50/1) to give the desired product **35**–**36**.

*6.1.22.1. 8-(benzo[d]thiazol-5-ylamino)-3-hydroxy-2,2,3-trimethyl-2,3-dihydrothieno[2,3-g]quinoline 1,1-dioxide (**35**).* Compound **35** was obtained as a yellow solid (30 mg, 52%)。$^1$H NMR (400 MHz, DMSO-$d_6$) δ 9.57 (s, 1H), 9.45 (s, 1H), 9.02 (s, 1H), 8.58 (d, $J$ = 5.6 Hz, 1H), 8.22 (d, $J$ = 8.4 Hz, 1H), 8.09 (s, 1H), 8.06 (s, 1H), 7.55 (d, $J$ = 8.4 Hz, 1H), 7.06 (d, $J$ = 5.2 Hz, 1H), 6.19 (s, 1H), 1.60 (s, 3H), 1.39 (s, 3H), 1.27 (s, 3H). $^{13}$C NMR (151 MHz, DMSO-$d_6$) δ 157.5, 154.1, 153.4, 151.2, 149.0, 144.8, 138.9, 132.1, 129.3, 125.0, 123.2, 121.5, 119.8, 117.8, 116.4, 101.9, 76.3, 67.1, 39.5, 26.6, 19.5, 15.5. HRMS (ESI) calcd for $C_{21}H_{19}N_3O_3S_2$, [M + H] $^+$, 426.0941, found, 426.0942. Purity: 97.5%.

*6.1.22.2. 8-(benzo[d]thiazol-5-ylamino)-3-cyclopropyl-3-hydroxy-2,2-dimethyl-2,3-dihydrothieno [2,3-g]quinoline 1,1-dioxide (**36**).* Compound **36** was obtained as a yellow solid (16 mg, 11%). $^1$H NMR (400 MHz, DMSO-$d_6$) δ 9.56 (s, 1H), 9.44 (s, 1H), 9.04 (s, 1H), 8.58 (d, $J$ = 5.2 Hz, 1H), 8.22 (d, $J$ = 8.4 Hz, 1H), 8.06 (s, 1H), 8.04 (s, 1H), 7.55 (d, $J$ = 8.4 Hz, 1H), 7.06 (d, $J$ = 5.2 Hz, 1H), 5.74 (s, 1H), 1.49 (s, 3H), 1.34–1.30 (m, 1H), 1.28 (s, 3H), 0.82–0.74 (m, 1H), 0.68–0.60 (m, 1H), 0.60–0.50 (m, 1H), 0.36–0.26 (m, 1H). $^{13}$C NMR (151 MHz, DMSO-$d_6$) δ 157.5, 154.1, 153.3, 150.8, 149.1, 143.9, 138.5, 132.4, 129.4, 125.5, 123.2, 121.5, 119.8, 117.7, 116.4, 101.9, 76.4, 68.0, 19.7, 18.2, 16.0, 2.1, −0.2. HRMS (ESI) calcd for $C_{23}H_{21}N_3O_3S_2$, [M + H] $^+$, 452.1097, found, 452.1097. Purity: 96.5%.

*6.1.23. 8-(benzo[d]thiazol-5-ylamino)-2,2-dimethyl-3-methylene-2,3-dihydrothieno[2,3-g]quinoline 1,1-dioxide (**37**)*

To a solution of methyltriphenylphosphonium bromide (260 mg, 0.73 mmol) in dry THF (5 mL) with $N_2$ atmosphere was added n-BuLi (0.33 mL, 0.83 mmol) dropwise at −78 °C. The reaction was stirred at 0 °C for 1.5 h. Then cooled to −78 °C, a solution of **26** (100 mg, 0.22 mmol) in THF (5 mL) was added and the mixture was stirred at room temperature overnight. Saturated $NH_4Cl$ aqueous solution was added to quench the solution and the

aqueous layer was extracted with EA (20 mL * 3). The combined organic phase was dried over $Na_2SO_4$, filtrated and concentrated. The residue was purified by silica gel column chromatography (DCM/MeOH = 20/1) to give the desired product **37** as a yellow solid (10 mg, 11%). $^1$H NMR (400 MHz, DMSO-$d_6$) δ 9.58 (s, 1H), 9.45 (s, 1H), 9.11 (s, 1H), 8.60 (d, $J$ = 5.2 Hz, 1H), 8.42 (s, 1H), 8.23 (d, $J$ = 8.8 Hz, 1H), 8.07 (s, 1H), 7.56 (d, $J$ = 8.4 Hz, 1H), 7.06 (d, $J$ = 5.2 Hz, 1H), 6.36 (s, 1H), 5.68 (s, 1H), 1.55 (s, 6H). $^{13}$C NMR (151 MHz, DMSO-$d_6$) δ 157.5, 154.1, 153.8, 151.2, 149.0, 144.0, 138.5, 133.8, 132.5, 129.4, 123.4, 123.2, 121.5, 120.5, 118.1, 116.5, 112.5, 102.0, 62.8, 21.8. HRMS (ESI) calcd for $C_{21}H_{17}N_3O_2S_2$, [M + H] $^+$, 408.0835. found 408.0835. Purity: 96.0%.

*6.1.24. General procedure for the synthesis of **38**–**39***

To a solution of **15b** (1 eq) in ethylene glycol or propane-1,2-diol (1 mmol/10 mL) was added $Cs_2CO_3$ (2.5 eq). The reaction was stirred at 60 °C for 5 h. The mixture was concentrated and purified by silica gel column chromatography (DCM/MeOH = 50/1) to give the desired product **38**–**39**.

*6.1.24.1. 8-(benzo[d]thiazol-5-ylamino)-2H-spiro[thieno[2,3-g]quinoline-3,2'- [1,3]dioxolane] 1,1-dioxide (**38**).* Compound **38** was obtained as a hydrochloride salt (55 mg, 13%)。 $^1$H NMR (400 MHz, DMSO-$d_6$) δ 15.02 (s, 1H), 11.48 (s, 1H), 9.55 (s, 1H), 9.46 (s, 1H), 8.63 (d, $J$ = 6.8 Hz, 1H), 8.40 (d, $J$ = 9.2 Hz, 1H), 8.38 (s, 1H), 8.25 (s, 1H), 7.63 (d, $J$ = 8.4 Hz, 1H), 6.99 (d, $J$ = 6.4 Hz, 1H), 4.38–4.30 (m, 2H), 4.28–4.20 (m, 2H), 4.14 (s, 2H). $^{13}$C NMR (151 MHz, DMOS-$d_6$) δ 158.6, 155.9, 154.0, 145.1, 142.1, 141.3, 138.1, 135.3, 133.1, 124.1, 122.9, 119.5, 119.3, 118.9, 117.1, 106.3, 101.3, 66.3, 59.8, 39.9, 39.8, 39.7, 39.5, 39.4, 39.2, 39.1. HRMS (ESI) calcd for $C_{20}H_{15}N_3O_4S_2$, [M + H] $^+$, 426.0577. found 426.0577. Purity: 98.8%.

*6.1.24.2. 8-(benzo[d]thiazol-5-ylamino)-4′-methyl-2H-spiro[thieno [2,3-g]quinoline-3,2'- [1,3] dioxolane] 1,1-dioxide (**39**).* Compound **39** was obtained as a yellow solid (15 mg, 7%). $^1$H NMR (400 MHz, DMSO-$d_6$) δ 9.64 (s, 1H), 9.45 (s, 1H), 9.08 (s, 1H), 8.62 (d, $J$ = 4.8 Hz, 1H), 8.23 (d, $J$ = 8.8 Hz, 1H), 8.13 (d, $J$ = 8.4 Hz, 1H), 8.08 (s, 1H), 7.56 (d, $J$ = 8.4 Hz, 1H), 7.09 (s, 1H), 4.75–4.26 (m, 2H), 4.20–3.91 (m, 2H), 3.91–3.65 (m, 1H), 1.53–1.29 (m, 3H). HRMS (ESI) calcd for $C_{21}H_{17}N_3O_4S_2$, [M + H] $^+$, 440.0733. found 440.0733. Purity: 99.7%.

*6.1.25. Methyl (E)-3-(5-nitrobenzo[b]thiophen-3-yl)acrylate (**40**)*

To a solution of **10** (5.0 g, 19.5 mmol) in DMF (50 mL) was added methyl acrylate (3.4 g, 39 mmol) , $NaHCO_3$ (3.3 g, 39 mmol), Xphos (954 mg, 2.0 mmol), $Pd(OAc)_2$ (220 mg, 1.0 mmol). The reaction was stirred at 120 °C under $N_2$ atmosphere for 4 h. The solvent was removed in vacuum and the residue was purified by silica gel column chromatography (DCM) to give the desired product **40** (3.6 g, 70%) as a yellow solid. $^1$H NMR (400 MHz, $CDCl_3$) δ 8.89 (s, 1H), 8.28 (d, $J$ = 8.0 Hz, 1H), 8.07–7.87 (m, 3H), 6.58 (d, $J$ = 16.0 Hz, 1H), 3.87 (s, 3H).

*6.1.26. 3-(5-aminobenzo[b]thiophen-3-yl)propan-1-ol (**41**)*

To a solution of **40** (3.6 g, 13.7 mmol) in dry THF (100 mL) with an ice bath was added $NaBH_4$ (4.2 g, 109.6 mmol) slowly. The reaction was stirred at room temperature overnight. $AlCl_3$ (3.6 g, 27.4 mmol) was added with an ice bath and the reaction was stirred at reflux temperature for 2 days. The reaction was quenched by saturated $NH_4Cl$ aqueous solution under ice bath. The solid was filtrated off, washed with EA (50 mL) and the resulting filtrate was extracted with EA (50 mL * 3). The combined organic phase was dried over $Na_2SO_4$, filtrated and concentrated. The residue was purified by silica gel column chromatography (DCM/MeOH = 50/1) to give the desired product **41** (1.8 g. 64%) as a yellow solid. $^1$H NMR (400 MHz, DMSO-$d_6$) δ 8.07 (s, 1H), 8.02 (d, $J$ = 8.4 Hz, 1H), 7.47 (d, $J$ = 8.4 Hz, 1H), 5.10 (s, 1H), 3.73–3.53 (m, 4H), 3.44–3.37 (m, 2H). LCMS (ESI/APCI) $m/z$: 207.9 [M + H] $^+$.

*6.1.27. 3-(3-hydroxypropyl)-5-nitrobenzo[b]thiophene 1,1-dioxide (**42**)*

To a solution of **41** (1.8 g, 8.7 mmol) in DCM (50 mL) with an ice bath was added 85% $m$-CPBA (4.4 g, 21.8 mmol). The mixture was stirred at room temperature overnight. The mixture was filtrated and the filtrate was quenched with $Na_2SO_3$, washed with saturated $NaHCO_3$ aqueous solution, extracted with DCM (40 mL * 3). The combined organic phase was dried over $Na_2SO_4$, filtrated and concentrated. The residue was purified by silica gel column chromatography (DCM/MeOH = 50/1) to give the desired product **42** (800 mg, 34%) as a yellow solid. $^1$H NMR (400 MHz, $CDCl_3$) δ 8.43 (d, $J$ = 7.6 Hz, 1H), 8.31 (s, 1H), 7.90 (d, $J$ = 8.0 Hz, 1H), 6.66 (s, 1H), 3.90–3.76 (m, 2H), 2.84 (t, $J$ = 6.8 Hz, 2H), 2.04–1.91 (m, 2H). LCMS (ESI/APCI) $m/z$: 267.8 [M - H] $^-$.

*6.1.28. 5-Nitro-4′,5′-dihydro-2H,3′H-spiro[benzo[b]thiophene-3,2′-furan] 1,1-dioxide (**43**)*

To a solution of **42** (800 mg, 3.0 mmol) in MeOH (40 mL) was added $Cs_2CO_3$ (1.47 g, 4.5 mmol). The mixture was turned into dark yellow quickly and stirred at room temperature for 2 h. The solvent was removed in vacuum and the residue was purified by silica gel column chromatography (PE/EA = 5/1) to give the desired product **43** (200 mg, 25%) as a yellow solid. $^1$H NMR (400 MHz, $CDCl_3$) δ 8.45–8.32 (m, 2H), 7.90 (d, $J$ = 8.4 Hz, 1H), 4.36–4.12 (m, 2H), 3.61 (q, $J$ = 13.0 Hz, 2H), 2.63–2.25 (m, 2H), 2.25–2.07 (m, 2H).

*6.1.29. 5-Amino-4′,5′-dihydro-2H,3′H-spiro[benzo[b]thiophene-3,2′-furan] 1,1-dioxide (**44**)*

To a solution of **43** (200 mg, 0.74 mmol) in EtOH (10 mL) and $H_2O$ (5 mL) was added iron powder (166 mg, 2.96 mmol) and $NH_4Cl$ (157 mg, 2.96 mmol). The mixture was stirred at 80 °C for 1 h. The solid was filtered off through diatomaceous earth and the cake was washed with DCM (100 mL). The resulting filtrate was extracted with DCM (20 mL * 3), dried over $Na_2SO_4$ and concentrated. The residue was purified by silica gel column chromatography (PE/EA = 1/1) to give the desired product **44** (120 mg, 68%) as a yellow solid. $^1$H NMR (400 MHz, $CDCl_3$) δ 7.47 (d, $J$ = 8.0 Hz, 1H), 6.71 (d, $J$ = 8.0 Hz, 1H), 6.66 (s, 1H), 4.18 (s, 2H), 4.15–4.04 (m, 2H), 3.46 (dd, $J$ = 41.6, 12.8 Hz, 2H), 2.56–2.16 (m, 3H), 2.16–2.01 (m, 2H). LCMS (ESI/APCI) $m/z$: 239.8 [M + H] $^+$.

*6.1.30. 5-(((1,1-Dioxido-4′,5′-dihydro-2H,3′H-spiro[benzo[b] thiophene-3,2′-furan]-5-yl)amino) methylene)-2,2-dimethyl-1,3-dioxane-4,6-dione (**45**)*

To a solution of **44** (120 mg, 0.5 mmol) in EtOH (5 mL) was added 5-(methoxymethylene)-2,2-dimethyl-1,3-dioxane-4,6-dione (140 mg, 0.75 mmol). The mixture was stirred at room temperature for 20 min. The resulting solid was collected via filtration, washed with EtOH (5 mL) and dried in vacuum to give the desired product **45** (140 mg 72%) as a yellow solid. $^1$H NMR (400 MHz, $CDCl_3$) δ 11.38 (d, $J$ = 13.6 Hz, 1H), 8.70 (d, $J$ = 13.6 Hz, 1H), 7.78 (d, $J$ = 8.0 Hz, 1H), 7.40 (s, 1H), 7.37 (d, $J$ = 8.8 Hz, 1H), 4.30–4.08 (m, 2H), 3.54 (dd, $J$ = 24.4, 12.8 Hz, 2H), 2.62–2.24 (m, 2H), 2.24–2.02 (m, 2H), 1.77 (s, 6H).

*6.1.31. 8′-hydroxy-4,5-dihydro-2′H,3H-spiro[furan-2,3′-thieno[2,3-g]quinoline] 1′,1′-dioxide (**46**)*

The diphenyl ether (10 mL) was added to a round-bottomed flask and the solvent was heated to 240 °C for 5 min. Intermediate **45** (140 mg, 0.36 mmol) was added slowly to the solution. The mixture was stirred for 5 min. After cooling to room temperature,

the resulting solid was collected via filtration, washed with ether (5 mL) and dried in vacuum to give the desired product **46** (52 mg, 50%) as a yellow solid. $^1$H NMR (400 MHz, DMSO-$d_6$) δ 12.08 (s, 1H), 8.29 (s, 1H), 8.03 (t, $J$ = 6.0 Hz, 1H), 7.73 (s, 1H), 6.14 (d, $J$ = 7.2 Hz, 1H), 4.13–4.00 (m, 2H), 3.97 (d, $J$ = 13.6 Hz, 1H), 3.61 (d, $J$ = 13.2 Hz, 1H), 2.46–2.37 (m, 1H), 2.23–2.11 (m, 3H). LCMS (ESI/APCI) $m/z$: 291.8 [M + H] $^+$.

#### 6.1.32. 8'-(benzo[d]thiazol-5-ylamino)-4,5-dihydro-2'H,3H-spiro[furan-2,3'-thieno[2,3-g]quinoline] 1',1'-dioxide (47)

Intermediate **46** (20 mg, 0.07 mmol) was added to $POCl_3$ (2 mL) and then the mixture was stirred at reflux for 2 h to afford a light brown solution. After cooling to room temperature, the excess $POCl_3$ was removed in vacuum. The residue was dissolved in EtOH (2 mL) and benzo[$d$]thiazol-5-amine (13 mg, 0.08) was added subsequently. The mixture was stirred at reflux for 2 h. After cooling to room temperature. the solid was precipitated out of the solution. The solid was collected via filtration, washed with EtOH and dried in vacuum to give the desired product **47** (15 mg, 51%) as a hydrochloride salt. $^1$H NMR (400 MHz, DMSO-$d_6$) δ 14.67 (s, 1H), 11.41 (s, 1H), 9.55 (s, 1H), 9.36 (s, 1H), 8.61 (d, $J$ = 6.4 Hz, 1H), 8.40 (d, $J$ = 8.4 Hz, 1H), 8.25 (s, 2H), 7.62 (d, $J$ = 8.0 Hz, 1H), 6.97 (d, $J$ = 6.8 Hz, 1H), 4.21–4.03 (m, 3H), 3.79 (d, $J$ = 13.5 Hz, 1H), 2.49–2.43 (m, 1H), 2.29–2.17 (m, 3H). $^{13}$C NMR (151 MHz, DMSO-$d_6$) δ 161.6, 158.5, 155.9, 153.9, 147.3, 144.7, 141.2, 137.4, 135.2, 132.9, 124.1, 122.9, 119.6, 118.6, 118.1, 116.4, 100.9, 83.4, 69.5, 61.4, 39.9, 39.8, 39.7, 39.5, 39.5, 39.4, 39.2, 39.1, 25.9. HRMS (ESI) calcd for $C_{21}H_{17}N_3O_3S_2$, [M + H] $^+$, 424.0784, found, 424.0784. Purity: 96.8%.

#### 6.1.33. Dimethyl 2-(2-fluorophenyl)malonate (49)

To a solution of **48** (10.3 g, 61.3 mmol) and dimethyl carbonate (16.6 g, 183.9 mmol) in dry THF (200 ml) with an ice bath was added 60% NaH (9.8 g, 245.2 mmol). The mixture was stirred at 70 °C overnight. The reaction was quenched by saturated $NH_4Cl$ aqueous solution with an ice bath. The aqueous layer was extracted with DCM (100 mL * 3). The combined organic phase was dried over $Na_2SO_4$, filtered and concentrated. The residue was purified by silica gel column chromatography (PE/EA = 20/1) to give the desired product **49** (11.2 g, 81%) as a yellow oil. $^1$H NMR (400 MHz, $CDCl_3$) δ 7.50–7.39 (m, 1H), 7.37–7.27 (m, 1H), 7.20–7.12 (m, 1H), 7.12–7.01 (m, 1H), 5.01 (s, 1H), 3.77 (s, 6H).

#### 6.1.34. Dimethyl 2-((benzyloxy)methyl)-2-(2-fluorophenyl) malonate (50)

To a solution of **49** (11.2 g, 49.6 mmol) and $Cs_2CO_3$ (32.3 g, 99.2 mmol) in DMF (130 mL) with an ice bath was added ((chloromethoxy)methyl)benzene (11.7 g, 74.4 mmol) dropwise. The mixture was stirred at room temperature for 1 h. The solvent was concentrated and water (400 mL) was added. The aqueous layer was extracted with EA (200 mL * 3). The combined organic phase was dried over $Na_2SO_4$, filtered and concentrated. The residue was purified by silica gel column chromatography (PE/EA = 20/1) to give the desired product **50** (12.6 g, 73%) as a colorless oil. $^1$H NMR (400 MHz, $CDCl_3$) δ 7.51–7.41 (m, 1H), 7.35–7.27 (m, 3H), 7.25–7.18 (m, 3H), 7.16–7.09 (m, 1H), 7.07–6.98 (m, 1H), 4.58 (s, 2H), 4.19 (s, 2H), 3.78 (s, 6H). LCMS (ESI/APCI) $m/z$: 346.8 [M + H] $^+$.

#### 6.1.35. 2-((benzyloxy)methyl)-2-(2-fluorophenyl)propane-1,3-diol (51)

To a solution of **50** (8.6 g, 24.9 mmol) in dry THF (100 mL) with an ice bath was added $LiAlH_4$ (3.8 g, 99.6 mmol) slowly. The reaction was stirred at room temperature for 2 h. The reaction mixture was cooled to 0 °C and $H_2O$ (3.8 mL) was added dropwise and stirred for 5 min then 15% NaOH sol. (3.8 mL) was added and stirred for 10 min after that $H_2O$ (11.4 mL) was added and stirred for 10 min. Precipitate was filtered off and washed with MeOH. The resulting filtrate was evaporated. The residue was purified by silica gel column chromatography (PE/EA = 2/1) to give the desired product **51** (1.8 g, 25%) as a colorless oil. $^1$H NMR (400 MHz, $CDCl_3$) δ 7.47–7.38 (m, 1H), 7.38–7.29 (m, 3H), 7.29–7.20 (m, 3H), 7.17–7.08 (m, 1H), 7.07–6.96 (m, 1H), 4.53 (s, 2H), 4.16 (d, $J$ = 11.2 Hz, 2H), 4.07 (d, $J$ = 10.4 Hz, 2H), 3.94 (s, 2H). LCMS (ESI/APCI) $m/z$: 290.9 [M + H] $^+$.

#### 6.1.36. 3-((benzyloxy)methyl)-3-(2-fluorophenyl)oxetane (52)

To a solution of **51** (1.8 g, 6.2 mmol) in dry THF (20 mL) with an ice bath under $N_2$ atmosphere was added n-BuLi (2.5 mL, 6.2 mmol) dropwise. The reaction was stirred at 0 °C for 10 min. A solution of $p$-TsCl (1.2 g, 6.2 mmol) in the THF (5 mL) was added and the mixture was stirred for 10 min at 0 °C. A solution of n-BuLi in hexanes (2.5 mL, 6.2 mmol) was added dropwise and the reaction was stirred at 55 °C overnight. The reaction mixture was cooled to 0 °C and saturated $NH_4Cl$ aqueous solution was added to quench the reaction. The mixture was extracted with EA (30 mL * 3). The combined organic phase was dried over $Na_2SO_4$, filtered and concentrated. The residue was purified by silica gel column chromatography (PE/EA = 20/1) to give the desired product **52** (1.1 g, 61%) as a colorless oil. $^1$H NMR (400 MHz, $CDCl_3$) δ 7.32–7.21 (m, 4H), 7.21–7.15 (m, 2H), 7.15–7.08 (m, 1H), 7.08–6.96 (m, 2H), 5.00 (d, $J$ = 5.6 Hz, 2H), 4.79 (d, $J$ = 5.2 Hz, 2H), 4.52 (s, 2H), 3.88 (s, 2H). LCMS (ESI/APCI) $m/z$: 272.9 [M + H] $^+$.

#### 6.1.37. (3-(2-fluorophenyl)oxetan-3-yl)methanol (53)

To a solution of **52** (1.1 g, 4.0 mmol) in MeOH (20 mL) was added 10% Pd/C (21 mg, 0.2 mmol). The reaction was stirred at room temperature under $H_2$ atmosphere for 12 h. The Pd/C was filtrated off and the cake was washed with MeOH. The resulting filtrate was concentrated to give the desired product **53** as a colorless oil (650 mg, 89%). $^1$H NMR (400 MHz, $CDCl_3$) δ 7.32–7.27 (m, 1H), 7.20–7.12 (m, 1H), 7.10–6.96 (m, 2H), 5.01 (d, $J$ = 6.0 Hz, 2H), 4.76 (d, $J$ = 6.0 Hz, 2H), 4.10 (s, 2H).

#### 6.1.38. 3-(chloromethyl)-3-(2-fluorophenyl)oxetane (54)

To a solution of **53** (420 mg, 2.3 mmol) in $CCl_4$ (20 mL) was added $PPh_3$ (1.2 g, 4.6 mmol). The reaction was stirred at 90 °C for 24 h. The solvent was removed in vacuum and the residue was purified by silica gel column chromatography (PE/EA = 40/1) to give the desired product **54** (440 mg, 96%) as a colorless oil. $^1$H NMR (400 MHz, $CDCl_3$) δ 7.34–7.27 (m, 1H), 7.16 (t, $J$ = 7.6 Hz, 1H), 7.10–6.99 (m, 2H), 5.02 (d, $J$ = 6.4 Hz, 2H), 4.74 (d, $J$ = 6.4 Hz, 2H), 4.11 (s, 2H).

#### 6.1.39. 3-(chloromethyl)-3-(2-fluoro-5-nitrophenyl)oxetane (55)

To a solution of **54** (440 mg, 2.2 mmol) in conc.$H_2SO_4$ (5 mL) with an ice bath was added fuming nitric acid (1 mL) dropwise. The reaction was stirred at room temperature for 5 min. The mixture was poured into cooled water (50 mL). The aqueous was extracted with EA (10 mL * 3). The combined organic phase was dried over $Na_2SO_4$, filtered and concentrated to give the desired product **55** (520 mg, 93%) as a yellow solid. $^1$H NMR (400 MHz, $CDCl_3$) δ 8.30–8.19 (m, 1H), 8.03–7.95 (m, 1H), 7.24–7.18 (m, 1H), 5.03 (d, $J$ = 5.2 Hz, 2H), 4.75 (d, $J$ = 5.6 Hz, 2H), 4.16 (s, 2H).

#### 6.1.40. 5-Nitro-2H-spiro[benzo[b]thiophene-3,3'-oxetane] (56)

To a solution of **55** (520 mg, 2.0 mmol) in DMSO (30 mL) was added $Na_2S.9H_2O$ (768 mg,3.2 mmol). The reaction was stirred at room temperature for 3 h. Water (80 mL) was added to the reaction and the aqueous was extracted with EA (20 mL * 2). The combined organic phase was dried over $Na_2SO_4$, filtered and concentrated. The residue was purified by silica gel column chromatography (PE/

EA = 10/1) to give the desired product **56** (240 mg, 51%) as a yellow sold. $^1$H NMR (400 MHz, $CDCl_3$) δ 8.43 (s, 1H), 8.11 (d, *J* = 8.8 Hz, 1H), 7.31 (d, *J* = 8.8 Hz, 1H), 4.85 (d, *J* = 6.4 Hz, 2H), 4.82 (d, *J* = 6.4 Hz, 2H), 3.78 (s, 2H).

#### 6.1.41. 5-Nitro-2H-spiro[benzo[b]thiophene-3,3′-oxetane] 1,1-dioxide (**57**)

To a solution of **56** (240 mg, 1.08 mmol) in DCM (15 mL) with an ice bath was added 85% *m*-CPBA (543 mg, 2.69 mmol). The mixture was stirred at room temperature overnight. The solid was filtered off and the filtrate was quenched with $Na_2SO_3$, extracted with DCM (20 mL * 3). The combined organic phase was washed with saturated $NaHCO_3$ aqueous solution, dried over $Na_2SO_4$, filtered and concentrated. The residue was purified by silica gel column chromatography (DCM/MeOH = 50/1) to give the desired product **57** (220 mg, 80%) as a white solid. $^1$H NMR (400 MHz, $CDCl_3$) δ 8.85 (s, 1H), 8.44 (d, *J* = 7.6 Hz, 1H), 7.92 (d, *J* = 8.4 Hz, 1H), 5.04 (d, *J* = 6.8 Hz, 2H), 4.95 (d, *J* = 6.8 Hz, 2H), 3.91 (s, 2H).

#### 6.1.42. 5-Amino-2H-spiro[benzo[b]thiophene-3,3′-oxetane] 1,1-dioxide (**58**)

To a solution of **57** (220 mg, 0.86 mmol) in EtOH (8 mL) and $H_2O$ (3 mL) was added iron powder (193 mg, 3.44 mmol) and $NH_4Cl$ (182 mg, 3.44 mmol). The mixture was stirred at 80 °C for 2 h. The solid was filtered through diatomaceous earth and the cake was washed with DCM. The resulting filtrate was extracted with DCM (20 mL * 2). The combined organic phase was dried over $Na_2SO_4$, filtrated and concentrated to give the desired product **58** (200 mg, 93%) as a yellow solid. $^1$H NMR (400 MHz, $CDCl_3$) δ 7.47 (d, *J* = 8.4 Hz, 1H), 7.10 (s, 1H), 6.74 (d, *J* = 8.0 Hz, 1H), 4.95 (d, *J* = 6.4 Hz, 2H), 4.87 (d, *J* = 6.0 Hz, 2H), 4.30 (s, 2H), 3.75 (s, 2H). LCMS (ESI/APCI) *m*/*z*: 225.8 [M + H] $^+$.

#### 6.1.43. 5-(((1,1-Dioxido-2H-spiro[benzo[b]thiophene-3,3′-oxetan]-5-yl)amino)methylene)-2,2-dimethyl−1,3-dioxane-4,6-dione (**59**)

To a solution of **58** (200 mg, 0.8 mmol) in EtOH (4 mL) was added 5-(methoxymethylene)-2,2-dimethyl-1,3-dioxane-4,6-dione (223 mg, 1.2 mmol). The mixture was stirred at room temperature for 20 min. The resulting solid was collected via filtration, washed with EtOH (5 mL) and dried in vacuum to give the desired product **59** (240 mg, 79%) as a yellow solid. $^1$H NMR (400 MHz, $CDCl_3$) δ 11.47 (d, *J* = 12.8 Hz, 1H), 8.76 (d, *J* = 13.6 Hz, 1H), 7.87−7.74 (m, 2H), 7.43 (d, *J* = 6.8 Hz, 1H), 5.03 (d, *J* = 6.0 Hz, 2H), 4.89 (d, *J* = 6.0 Hz, 2H), 3.84 (s, 2H), 1.79 (s, 6H).

#### 6.1.44. 8′-hydroxy-2′H-spiro[oxetane-3,3′-thieno[2,3-g]quinoline] 1′,1′-dioxide (**60**)

The diphenyl ether (6 mL) was added to a round-bottomed flask and the solvent was heated to 240 °C for 5 min. Intermediate **59** (240 mg, 0.63 mmol) was added slowly to the solution. The mixture was stirred for 5 min. After cooling to room temperature, the resulting suspension was then filtered, washed with ether (2 mL) and dried in vacuum to give the desired product **60** (110 mg, 63%) as a yellow solid. $^1$H NMR (400 MHz, DMSO-$d_6$) δ 12.34 (s, 1H), 8.27 (s, 1H), 8.17 (s, 1H), 8.05 (d, *J* = 7.6 Hz, 1H), 6.15 (d, *J* = 7.2 Hz, 1H), 4.96 (d, *J* = 6.0 Hz, 2H), 4.77 (d, *J* = 6.4 Hz, 2H), 4.13 (s, 2H). LCMS (ESI/APCI) *m*/*z*: 277.8 [M + H] $^+$.

#### 6.1.45. 8′-(benzo[d]thiazol-5-ylamino)-2′H-spiro[oxetane-3,3′-thieno[2,3-g]quinoline] 1′,1′-dioxide (**61**)

To a solution of **60** (30 mg, 0.11 mmol) and pyridine (0.1 mL, 1.0 mmol) in dry DCM (4 mL) was added trifluoromethanesulfonic anhydride (0.1 mL, 0.6 mmol) dropwise at 0 °C. The reaction was stirred at room temperature for 30 min. The solvent was removed in vacuum and the residue was dissolved in dioxane (4 mL) subsequently. $Pd_2(dba)_3$ (18 mg, 0.02 mmol), Xantphos (12 mg, 0.02 mmol), $Cs_2CO_3$ (359 mg, 1.1 mmol) was added. The reaction was stirred at 100 °C for 1 h under $N_2$ atmosphere. The solvent was removed in vacuum and the resulting residue was purified by silica gel column chromatography (DCM/MeOH = 20/1) to give the desired product **61** (15 mg, 33%) as a yellow solid. $^1$H NMR (400 MHz, DMSO-$d_6$) δ 9.59 (s, 1H), 9.45 (s, 1H), 8.99 (s, 1H), 8.63 (d, *J* = 5.6 Hz, 1H), 8.47 (s, 1H), 8.23 (d, *J* = 8.8 Hz, 1H), 8.07 (d, *J* = 1.7 Hz, 1H), 7.56 (dd, *J* = 8.8, 1.6 Hz, 1H), 7.09 (d, *J* = 5.6 Hz, 1H), 4.97 (d, *J* = 6.4 Hz, 2H), 4.94 (d, *J* = 6.4 Hz, 2H), 4.23 (s, 2H). $^{13}$C NMR (151 MHz, DMSO-$d_6$) δ 157.5, 154.1, 153.6, 151.5, 149.2, 141.2, 138.5, 135.2, 129.4, 124.9, 123.2, 121.5, 119.6, 116.7, 116.4, 102.1, 80.7, 59.3, 43.9, 39.9, 39.8, 39.7, 39.5, 39.5, 39.4, 39.2, 39.1. HRMS (ESI) calcd for $C_{20}H_{15}N_3O_3S_2$, [M + H] $^+$, 410.0628, found, 410.0628. Purity: 98.3%.

### 6.2. In vitro biological assays

#### 6.2.1. Cell culture

Human colon cancer HT-29 (from ATCC) and mouse embryonic fibroblasts (MEFs) were cultured in Dulbecco's modified Eagle's medium (Hyclone) supplemented with 10% fetal bovine serum (Invitrogen), 2 mM L-glutamine (Invitrogen) and 100-units/ml penicillin/streptomycin (Hyclone) in a humidified incubator at 37 °C and 5% $CO_2$.

#### 6.2.2. Cell viability assay

HT-29 cells or MEFs seeded in 96-well plates were treated with or without the indicated compound for 1h prior to the treatment of DMSO or TNFα, Smac mimetic and z-VAD (Bachem). After 24h, the cell viability was determined by assessment of ATP levels using the CellTiter-Glo Luminescent Cell Viability Assay kit (Promega). Luminescence was measured with SpectraMax i3x (Molecular Devices). Smac mimetic was kindly provided by Dr. Xiaodong Wang (National Institute of Biological Sciences, Beijing).

#### 6.2.3. Kinase binding ($K_d$) assay [45]

The binding affinity of the test compounds for kinases was detected by a KINOMEscan assay. Kinase-tagged T7 phage strains were prepared in an *E. coli* host derived from the BL21 strain. *E. coli* were grown to log-phase and infected with T7 phage and incubated with shaking at 32 °C until lysis. The lysates were centrifuged and filtered to remove cell debris. The remaining kinases were produced in HEK-293 cells and subsequently tagged with DNA for qPCR detection. Streptavidin-coated magnetic beads were treated with biotinylated small molecule ligands for 30 min at room temperature to generate affinity resins for kinase assays. The liganded beads were blocked with excess biotin and washed with blocking buffer (SeaBlock (Pierce), 1% BSA, 0.05% Tween 20, 1 mM DTT) to remove unbound ligand and to reduce non-specific binding. Binding reactions were assembled by combining kinases, liganded affinity beads, and test compounds in 1x binding buffer (20% SeaBlock, 0.17x PBS, 0.05% Tween 20, 6 mM DTT). All reactions were performed in polypropylene 384-well plate. Each was a final volume of 0.02 ml. The assay plates were incubated at room temperature with shaking for 1 h and the affinity beads were washed with wash buffer (1x PBS, 0.05% Tween 20). The beads were then resuspended in elution buffer (1x PBS, 0.05% Tween 20, 0.5 μM non-biotinylated affinity ligand) and incubated at room temperature with shaking for 30 min. The kinase concentration in the eluates was measured by qPCR.

#### 6.2.4. Kinase functional activity assay

*6.2.4.1. ADP-Glo Luminescent Assay.* Inhibition of ALK4, PI3Kα, RIPK1 or RIPK3 was determined using an ADP-Glo Luminescent Assay. Kinase was incubated with the indicated compound or

DMSO for around 15 min in the assay buffer (20 mM $MgCl_2$, 25 mM HEPES pH 7.2, 12.5 mM β-glycerol phosphate, 5 mM EGTA, 12.5 mM $MnCl_2$, 2 mM EDTA and 2 mM DTT for RIPK1 and RIPK3; 40 mM Tris, pH 7.5 20 mM MgCl2,1 mM DTT, 0.10%BSA for ALK4; 50 mM HEPES, pH 7.5, 3 mM MgCl2, 1 mM EGTA,0.03%CHAPS, 100 mM NaCl,2 mM DTT for PI3Kα). Substrate and ATP (50 μM for RIPK1, RIPK3; Km for ALK4; 25 μM for PI3Kα) were added and the mixture was incubated at room temperature (120 min for ALK4, RIPK1, RIPK3 and 60 min for PI3Kα). The luminescence was calculated to determine the kinase activity using the ADP-Glo Kinase Assay kit following the manufacture's instructions (Promega).

*6.2.4.2. Mobility shift assay.* Inhibition of EGFR, PDGFRa or CDK4/CycD3 was determined using a mobility shift assay. Kinase was incubated with the indicated compound for 10 min at room temperature. FAM-labeled peptide and ATP (Km) were added and the mixture was incubated at 28 °C for 60 min on the 384-well assay plate. Data was collected on Caliper.

*6.2.4.3. Lance Ultra Assay.* Inhibition of m-TOR protein kinase was determined using a Lance Ultra Assay. Kinase was incubated with the indicated compound in the assay buffer (50 mM HEPES, pH 7.5, 10 mM $MgCl_2$, 3 mM $MnCl_2$, 1 mM EGTA, 0.01% Tween-20). ATP (Km) and substrate were added and the mixture was incubated at 28 °C for 60 min on the 384-well assay plate. Kinase quench buffer and antibody were prepared as detection solution and the solution was added to the reaction. After 60 min at room temperature, values of Lance signal ratio were collected from Envision program (665nm/615 nm) and converted to percent inhibition values.

*6.2.4.4. Lantha screen assay.* Inhibition of BRAF protein kinase was determined using a TR-FRET–based LanthaScreen method. Compounds were assayed at a maximum concentration of 10 μmol/L in the presence of ATP at Km. Data was collected on Envision with excitation at 340 nm and emission at 520nm/495 nm and converted to percent inhibition values.

### 6.3. Preliminary in vitro safety and DMPK test

- Evaluation of CYP inhibitory potency [46]
  - •hERG assays [47]
  - •Metabolic stability test [48]
  - •Plasma protein binding (PPB) assay [49]

### 6.4. Animal experiments

#### 6.4.1. TNF-induced systemic inflammatory response syndrome

Compound **38** was diluted into sterile PBS containing 40% PEG400. C57BL/6 mice were purchased from Beijing Vital River Laboratory. C57BL/6 mice were pretreated with vehicle or compound **38** (5 mg/kg) via intraperitoneal injection for around 15 min prior to the tail intravenous injection of mouse TNF-α (0.35 μg/g per mouse). The body temperature and survival rate were monitored. The body temperature changes (means ± SEM) for each group were shown. To measure TNFα-induced IL-6 level in serum, the mice were scarified 4h post TNFα injection and serum was collected for analysis of IL-6 by using Mouse IL-6 ELISA kit (MultiSciences, Lianke). Data are represented as the mean ± standard deviation. P-values were determined using TWO-way ANOVA or multi-comparison test for statistics analysis. *$P < 0.05$, **$P < 0.01$, ***$P < 0.001$.

## Declaration of competing interest

Sudan He and Xiaohu Zhang of the manuscript entitled "Ring Closure Strategy Leads to Potent RIPK3 Inhibitors" declare the following conflict of interest: S. He and X. Zhang are co-founders, consultants and shareholders of Accro Bioscience Inc., which supports research in their labs.

## Acknowledgements

This work was supported by National Natural Science Foundation of China (Grant No. 81973161, 81773561, 21502133, 31671436, 31830051), the Priority Academic Program Development of the Jiangsu Higher Education Institutes (PAPD), the Jiangsu Key Laboratory of Neuropsychiatric Diseases (BM2013003), the CAMS Innovation Fund for Medical Sciences (CIFMS; 2019-I2M-1–004, 2019-I2M-1–003, and 2016-I2M-1–005) and Non-profit Central Research Institute Fund of Chinese Academy of Medical Sciences (2019PT310028, 2017NL31004, 2017NL31002). We are grateful to Prof. Youyong Li in the Institute of Functional Nano & Soft Materials (FUNSOM) at Soochow University for providing Schrodinger software for molecular docking.

## Appendix A. Supplementary data

Supplementary data to this article can be found online at https://doi.org/10.1016/j.ejmech.2021.113327.

## References

[1] M. Jaattela, J. Tschopp, Caspase-independent cell death in T lymphocytes, Nat. Immunol. 4 (2003) 416–423.
[2] Y.K. Dhuriya, D. Sharma, Necroptosis: a regulated inflammatory mode of cell death, J. Neuroinflammation 15 (2018).
[3] P. Vandenabeele, L. Galluzzi, T. Vanden Berghe, G. Kroemer, Molecular mechanisms of necroptosis: an ordered cellular explosion, Nat. Rev. Mol. Cell Biol. 11 (2010) 700–714.
[4] S.D. He, Y.Q. Liang, F. Shao, X.D. Wang, Toll-like receptors activate programmed necrosis in macrophages through a receptor-interacting kinase-3-mediated pathway, P Natl Acad Sci USA 108 (2011) 20054–20059.
[5] E.J. Petrie, P.E. Czabotar, J.M. Murphy, The structural basis of necroptotic cell death signaling, Trends Biochem. Sci. 44 (2019) 53–63.
[6] Y. Cho, S. Challa, D. Moquin, R. Genga, T.D. Ray, M. Guildford, F.K.M. Chan, Phosphorylation-driven assembly of the RIP1-RIP3 complex regulates programmed necrosis and virus-induced inflammation, Cell 137 (2009) 1112–1123.
[7] S.D. He, L. Wang, L. Miao, T. Wang, F.H. Du, L.P. Zhao, X.D. Wang, Receptor interacting protein kinase-3 determines cellular necrotic response to TNF-alpha, Cell 137 (2009) 1100–1111.
[8] L.M. Sun, H.Y. Wang, Z.G. Wang, S.D. He, S. Chen, D.H. Liao, L. Wang, J.C. Yan, W.L. Liu, X.G. Lei, X.D. Wang, Mixed lineage kinase domain-like protein mediates necrosis signaling downstream of RIP3 kinase, Cell 148 (2012) 213–227.
[9] J. Zhao, S. Jitkaew, Z.Y. Cai, S. Choksi, Q.N. Li, J. Luo, Z.G. Liu, Mixed lineage kinase domain-like is a key receptor interacting protein 3 downstream component of TNF-induced necrosis, P Natl Acad Sci USA 109 (2012) 5322–5327.
[10] Z. Cai, S. Jitkaew, J. Zhao, H.C. Chiang, S. Choksi, J. Liu, Y. Ward, L.G. Wu, Z.G. Liu, Plasma membrane translocation of trimerized MLKL protein is required for TNF-induced necroptosis, Nat. Cell Biol. 16 (2014) 55–65.
[11] H. Wang, L. Sun, L. Su, J. Rizo, L. Liu, L.F. Wang, F.S. Wang, X. Wang, Mixed lineage kinase domain-like protein MLKL causes necrotic membrane disruption upon phosphorylation by RIP3, Mol. Cell 54 (2014) 133–146.
[12] X. Chen, W. Li, J. Ren, D. Huang, W.T. He, Y. Song, C. Yang, W. Li, X. Zheng, P. Chen, J. Han, Translocation of mixed lineage kinase domain-like protein to plasma membrane leads to necrotic cell death, Cell Res. 24 (2014) 105–121.
[13] J.M. Murphy, P.E. Czabotar, J.M. Hildebrand, I.S. Lucet, J.G. Zhang, S. Alvarez-Diaz, R. Lewis, N. Lalaoui, D. Metcalf, A.I. Webb, S.N. Young, L.N. Varghese, G.M. Tannahill, E.C. Hatchell, I.J. Majewski, T. Okamoto, R.C. Dobson, D.J. Hilton, J.J. Babon, N.A. Nicola, A. Strasser, J. Silke, W.S. Alexander, The pseudokinase MLKL mediates necroptosis via a molecular switch mechanism, Immunity 39 (2013) 443–453.
[14] P.S. Welz, A. Wullaert, K. Vlantis, V. Kondylis, V. Fernandez-Majada, M. Ermolaeva, P. Kirsch, A. Sterner-Kock, G. van Loo, M. Pasparakis, FADD prevents RIP3-mediated epithelial cell necrosis and chronic intestinal

inflammation, Nature 477 (2011) 330–334.
[15] A. Linkermann, J.H. Brasen, F. De Zen, R. Weinlich, R.A. Schwendener, D.R. Green, U. Kunzendorf, S. Krautwald, Dichotomy between RIP1- and RIP3-mediated necroptosis in tumor necrosis factor-alpha-induced shock, Mol. Med. 18 (2012) 577–586.
[16] D. Ofengeim, Y. Ito, A. Najafov, Y. Zhang, B. Shan, J.P. DeWitt, J. Ye, X. Zhang, A. Chang, H. Vakifahmetoglu-Norberg, J. Geng, B. Py, W. Zhou, P. Amin, J. Berlink Lima, C. Qi, Q. Yu, B. Trapp, J. Yuan, Activation of necroptosis in multiple sclerosis, Cell Rep. 10 (2015) 1836–1849.
[17] M. Pasparakis, P. Vandenabeele, Necroptosis and its role in inflammation, Nature 517 (2015) 311–320.
[18] L. Seifert, G. Werba, S. Tiwari, L.N.N. Giao, D. Alqunaibit, S. Alothman, D. Daley, M. Hundeyin, V.R. Mani, R. Barilla, G. Miller, The necrosome promotes pancreatic Oncogenesis via CXCL1 and mincle-induced immune Suppression, Canc. Res. 76 (2016).
[19] H. Yang, Y.T. Ma, G. Chen, H. Zhou, T. Yamazaki, C. Klein, F. Pietrocola, E. Vacchelli, S. Souquere, A. Sauvat, L. Zitvogel, O. Kepp, G. Kroemer, Contribution of RIP3 and MLKL to immunogenic cell death signaling in cancer chemotherapy, OncoImmunology 5 (2016).
[20] A. Caccamo, C. Branca, I.S. Piras, E. Ferreira, M.J. Huentelman, W.S. Liang, B. Readhead, J.T. Dudley, E.E. Spangenberg, K.N. Green, R. Belfiore, W. Winslow, S. Oddo, Necroptosis activation in Alzheimer's disease, Nat. Neurosci. 20 (2017) 1236–1246.
[21] R. Weinlich, A. Oberst, H.M. Beere, D.R. Green, Necroptosis in development, inflammation and disease, Nat. Rev. Mol. Cell Biol. 18 (2017) 127–136.
[22] C.D. Guibao, K. Petrinjak, T. Moldoveanu, Uncovering human mixed lineage kinase domain-like activation in necroptosis, Future Med. Chem. 11 (2019) 2831–2844.
[23] Y.P. Liu, T. Liu, T.T. Lei, D.D. Zhang, S.Y. Du, L. Girani, D.D. Qi, C. Lin, R.S. Tong, Y. Wang, RIP1/RIP3-regulated necroptosis as a target for multifaceted disease therapy (Review), Int. J. Mol. Med. 44 (2019) 771–786.
[24] L. Mifflin, D. Ofengeim, J. Yuan, Receptor-interacting protein kinase 1 (RIPK1) as a therapeutic target, Nat. Rev. Drug Discov. 19 (2020) 553–571.
[25] D. Ofengeim, J.Y. Yuan, Regulation of RIP1 kinase signalling at the crossroads of inflammation and cell death, Nat. Rev. Mol. Cell Biol. 14 (2013) 727–736.
[26] Z. Cai, Z.G. Liu, Execution of RIPK3-regulated necrosis, Mol Cell Oncol 1 (2014), e960759.
[27] J. Boudeau, D. Miranda-Saavedra, G.J. Barton, D.R. Alessi, Emerging roles of pseudokinases, Trends Cell Biol. 16 (2006) 443–452.
[28] J.M. Murphy, P.E. Czabotar, J.M. Hildebrand, I.S. Lucet, J.G. Zhang, S. Alvarez-Diaz, R. Lewis, N. Lalaoui, D. Metcalf, A.I. Webb, S.N. Young, L.N. Varghese, G.M. Tannahill, E.C. Hatchell, I.J. Majewski, T. Okamoto, R.C.J. Dobson, D.J. Hilton, J.J. Babon, N.A. Nicola, A. Strasser, J. Silke, W.S. Alexander, The pseudokinase MLKL mediates necroptosis via a molecular switch mechanism, Immunity 39 (2013) 443–453.
[29] A. Takaoka, Z. Wang, M.K. Choi, H. Yanai, H. Negishi, T. Ban, Y. Lu, M. Miyagishi, T. Kodama, K. Honda, Y. Ohba, T. Taniguchi, DAI (DLM-1/ZBP1) is a cytosolic DNA sensor and an activator of innate immune response, Nature 448 (2007) 501–U514.
[30] J.X. Li, J.M. Feng, Y. Wang, X.H. Li, X.X. Chen, Y. Su, Y.Y. Shen, Y. Chen, B. Xiong, C.H. Yang, J. Ding, Z.H. Miao, The B-Raf(V600E) inhibitor dabrafenib selectively inhibits RIP3 and alleviates acetaminophen-induced liver injury, Cell Death Dis. 5 (2014).
[31] A. Fauster, M. Rebsamen, K.V. Huber, J.W. Bigenzahn, A. Stukalov, C.H. Lardeau, S. Scorzoni, M. Bruckner, M. Gridling, K. Parapatics, J. Colinge, K.L. Bennett, S. Kubicek, S. Krautwald, A. Linkermann, G. Superti-Furga, A cellular screen identifies ponatinib and pazopanib as inhibitors of necroptosis, Cell Death Dis. 6 (2015) e1767.
[32] S.A. Cruz, Z.H. Qin, A.F.R. Stewart, H.H. Chen, Dabrafenib, an inhibitor of RIP3 kinase-dependent necroptosis, reduces ischemic brain injury, Neural Regen Res 13 (2018) 252–256.
[33] H. Zhang, L. Xu, X. Qin, X. Chen, H. Cong, L. Hu, L. Chen, Z. Miao, W. Zhang, Z. Cai, C. Zhuang, N-(7-Cyano-6-(4-fluoro-3-(2-(3-(trifluoromethyl)phenyl) acetamido)phenoxy)benzo[d] thiazol-2-yl)cyclopropanecarboxamide (TAK-632) analogues as novel necroptosis inhibitors by targeting receptor-interacting protein kinase 3 (RIPK3): synthesis, structure-activity relationships, and in vivo efficacy, J. Med. Chem. 62 (2019) 6665–6681.
[34] A.C. Hart, L. Abell, J. Guo, M.E. Mertzman, R. Padmanabha, J.E. Macor, C. Chaudhry, H. Lu, K. O'Malley, P.J. Shaw, C. Weigelt, M. Pokross, K. Kish, K.S. Kim, L. Cornelius, A.E. Douglas, D. Calambur, P. Zhang, B. Carpenter, W.J. Pitts, Identification of RIPK3 type II inhibitors using high-throughput mechanistic studies in hit triage, ACS Med. Chem. Lett. 11 (2020) 266–271.
[35] P. Mandal, S.B. Berger, S. Pillay, K. Moriwaki, C.Z. Huang, H.Y. Guo, J.D. Lich, J. Finger, V. Kasparcova, B. Votta, M. Ouellette, B.W. King, D. Wisnoski, A.S. Lakdawala, M.P. DeMartino, L.N. Casillas, P.A. Haile, C.A. Sehon, R.W. Marquis, J. Upton, L.P. Daley-Bauer, L. Roback, N. Ramia, C.M. Dovey, J.E. Carette, F.K.M. Chan, J. Bertin, P.J. Gough, E.S. Mocarski, W.J. Kaiser, RIP3 induces apoptosis independent of pronecrotic kinase activity, Mol. Cell 56 (2014) 481–495.
[36] T. Xie, W. Peng, C.Y. Yan, J.P. Wu, X.Q. Gong, Y.G. Shi, Structural insights into RIP3-mediated necroptotic signaling, Cell Rep. 5 (2013) 70–78.
[37] H.M. Berman, J. Westbrook, Z. Feng, G. Gilliland, T.N. Bhat, H. Weissig, I.N. Shindyalov, P.E. Bourne, The protein Data Bank, Nucleic Acids Res. 28 (2000) 235–242.
[38] Schrödinger, version 9.0, L.L.C. Schrödinger, New York, 2009, http://www.schrodinger.com.
[39] W.F. Lu, D.H. Zhang, H.K. Ma, S. Tian, J.Y. Zheng, Q. Wang, L.S. Luo, X.H. Zhang, Discovery of potent and novel smoothened antagonists via structure-based virtual screening and biological assays, Eur. J. Med. Chem. 155 (2018) 34–48.
[40] F. Zhu, Y.J. Wang, Q. Du, W.X. Ge, Z.H. Li, X. Wang, C.Y. Fu, L.S. Luo, S. Tian, H.K. Ma, J.Y. Zheng, Y. Zhang, X.T. Sun, S.D. He, X.H. Zhang, Structural optimization of aminopyrimidine-based CXCR4 antagonists, Eur. J. Med. Chem. 187 (2020).
[41] P.A. Haile, L.N. Casillas, M.J. Bury, J.F. Mehlmann, R. Singhaus, A.K. Charnley, T.V. Hughes, M.P. DeMartino, G.Z. Wang, J.J. Romano, X.Y. Dong, N.V. Plotnikov, A.S. Lakdawala, M.A. Convery, B.J. Votta, D.B. Lipshutz, B.M. Desai, B. Swift, C.A. Capriotti, S.B. Berger, M.K. Mahajan, M.A. Reilly, E.J. Rivera, H.H. Sun, R. Nagilla, C. LePage, M.T. Ouellette, R.D. Totoritis, B.T. Donovan, B.S. Brown, K.W. Chaudhary, P.J. Gough, J. Bertin, R.W. Marquis, Identification of quinoline-based RIP2 kinase inhibitors with an improved therapeutic index to the hERG ion channel, ACS Med. Chem. Lett. 9 (2018) 1039–1044.
[42] P.A. Haile, B.J. Votta, R.W. Marquis, M.J. Bury, J.F. Mehlmann, R. Singhaus, A.K. Charnley, A.S. Lakdawala, M.A. Convery, D.B. Lipshutz, B.M. Desai, B. Swift, C.A. Capriotti, S.B. Berger, M.K. Mahajan, M.A. Reilly, E.J. Rivera, H.H. Sun, R. Nagilla, A.M. Beal, J.N. Finger, M.N. Cook, B.W. King, M.T. Ouellette, R.D. Totoritis, M. Pierdomenico, A. Negroni, L. Stronati, S. Cucchiara, B. Ziolkowski, A. Vossenkamper, T.T. MacDonald, P.J. Gough, J. Bertin, L.N. Casillas, The identification and pharmacological characterization of 6-(tert-Butylsulfonyl)-N-(5-fluoro-1H-indazol-3-yl)quinolin-4-amine (GSK583), a highly potent and selective inhibitor of RIP2 kinase, J. Med. Chem. 59 (2016) 4867–4880.
[43] L. Duprez, N. Takahashi, F. Van Hauwermeiren, B. Vandendriessche, V. Goossens, T. Vanden Berghe, W. Declercq, C. Libert, A. Cauwels, P. Vandenabeele, RIP kinase-dependent necrosis drives lethal systemic inflammatory response syndrome, Immunity 35 (2011) 908–918.
[44] S.B. Berger, V. Kasparcova, S. Hoffman, B. Swift, L. Dare, M. Schaeffer, C. Capriotti, M. Cook, J. Finger, A. Hughes-Earle, P.A. Harris, W.J. Kaiser, E.S. Mocarski, J. Bertin, P.J. Gough, Cutting Edge: RIP1 kinase activity is dispensable for normal development but is a key regulator of inflammation in SHARPIN-deficient mice, J. Immunol. 192 (2014) 5476–5480.
[45] M.A. Fabian, W.H. Biggs, D.K. Treiber, C.E. Atteridge, M.D. Azimioara, M.G. Benedetti, T.A. Carter, P. Ciceri, P.T. Edeen, M. Floyd, J.M. Ford, M. Galvin, J.L. Gerlach, R.M. Grotzfeld, S. Herrgard, D.E. Insko, M.A. Insko, A.G. Lai, J.M. Lelias, S.A. Mehta, Z.V. Milanov, A.M. Velasco, L.M. Wodicka, H.K. Patel, P.P. Zarrinkar, D.J. Lockhart, A small molecule-kinase interaction map for clinical kinase inhibitors, Nat. Biotechnol. 23 (2005) 329–336.
[46] A. Chen, X.J. Zhou, S.W. Tang, M.Y. Liu, X. Wang, Evaluation of the inhibition potential of plumbagin against cytochrome P450 using LC-MS/MS and cocktail approach, Sci Rep-Uk 6 (2016).
[47] J. Kutchinsky, S. Friis, M. Asmild, R. Taboryski, S. Pedersen, R.K. Vestergaard, R.B. Jacobsen, K. Krzywkowski, R.L. Schroder, T. Ljungstrom, N. Helix, C.B. Sorensen, M. Bech, N.J. Willumsen, Characterization of potassium channel modulators with QPatch (TM) automated patch-clamp technology: system characteristics and performance, Assay Drug Dev. Technol. 1 (2003) 685–693.
[48] R. Bera, A. Kundu, T. Sen, D. Adhikari, S. Karmakar, In vitro metabolic stability and permeability of gymnemagenin and its in vivo pharmacokinetic correlation in rats - a pilot study, Planta Med. 82 (2016) 544–550.
[49] H. Wan, M. Rehngren, High-throughput screening of protein binding by equilibrium dialysis combined with liquid chromatography and mass spectrometry, J. Chromatogr. A 1102 (2006) 125–134.